



UPPSALA
UNIVERSITET

ISRN UTH-INGUTB-EX-E-2012/05-SE

Examensarbete 15 hp
Maj 2012

**Design and Simulation of Field Oriented
Control and Direct Torque Control for a
Permanent Magnet Synchronous Motor with
Positive Saliency**

Anders Kronberg



UPPSALA
UNIVERSITET

**Teknisk- naturvetenskaplig fakultet
UTH-enheten**

Besöksadress:
Ångströmlaboratoriet
Lägerhyddsvägen 1
Hus 4, Plan 0

Postadress:
Box 536
751 21 Uppsala

Telefon:
018 – 471 30 03

Telefax:
018 – 471 30 00

Hemsida:
<http://www.teknat.uu.se/student>

Abstract

Design and Simulation of Field Oriented Control and Direct Torque Control for a Permanent Magnet Synchronous Motor with Positive Saliency

Anders Kronberg

The researchers at the Department of Electricity at Uppsala University has recently entered the field of electric motor design, however no real knowledge of motor control of salient pole permanent magnet motors exists in the department. This thesis will present a general description of the control method of motors that exist today, this has been done by reviewing existing literature. The literature review has shown that there are at least three control methods with a significant different in their control approach, Scalar-, Field Oriented- and Direct Torque- Control. The two last methods were chosen by the author as the most useful and was implemented and simulated together with the newly developed motor in MATLAB Simulink to evaluate their performance. The simulation results show that there is no difference in performance of the two methods, but they show a difference in efficiency.

The results show that it's worth to develop both methods further, mainly for reducing the torque and current ripple. This result was not expected according to literature, which suggests that the Field Oriented Control has a lower torque ripple. This could be caused by the choice of hysteresis control for inverter switching, instead of more sophisticated methods with a proportional integral derivative controller (PID) together with Sinusoidal Pulse Width Modulation (SPWM) or Space Vector Modulation (SVM).

Handledare: Boel Ekergård
Ämnesgranskare: Janaína Gonçalves
Examinator: Nora Masszi
ISRN UTH-INGUTB-EX-E-2012/05-SE

Motorstyrning av elmotorer med utpräglade poler

En jämförande studie och simulering av två olika metoder för styrning av elektriska motorer visar att prestanda skillnaden mellan dem är liten, men att de skiljer sig i strömförbrukning och därmed effektivitet. Båda metoderna har visat sig ha ett högt pulserande vridmoment, vilket kan ge sämre hållfasthet på den mekaniska sidan. Slutsatsen är att det med mer utveckling går att minska det pulserande vridmomentet och öka effektiviteten för motorstyrningen.

Med stigande oljepriser och en ökad miljömedvetenhet, kommer elektriska fordon att utgöra en allt större del av marknaden för persontransport, syftet med studien har varit att undersöka vilka kontrollmetoder för elektriska motorer som kan vara lämpliga för framdrivning av elfordon.

En av elbilens nackdelar är dess räckvidd, för att kunna konkurrera med dagens bilar är det därför viktigt att optimera verkningsgraden i de olika delsystemen mellan laddkontakt och hjul.

Studien har gjorts genom att undersöka de olika kontrollmetoder som finns beskrivna i existerande litteratur och två av dem valdes ut för en mer noggrann genomgång. De två valdes p.g.a. den stora skillnaden i kontrollmetod, den ena använder sig av en matematisk modell och positionsmätning av motorn för att generera styrsignaler, den andra av en uppskattning av motorn position från dess elektriska parametrar.

De två metoderna har sedan simulerats i Simulink för att kunna uppskatta deras skillnader och likheter i beteende och prestanda. Simulink är ett tillägg till Matlab vilket möjliggör att snabbt och enkelt kunna simulera bl.a. elektriska system genom att grafiskt koppla samman olika komponentblock till ett större system.

Contents

1	Introduction	1
1.1	Introduction	1
1.2	Motivation	1
1.3	Purpose	2
1.4	Thesis Outline	2
2	Permanent Magnet Synchronous Motors	3
2.1	Introduction	3
2.2	Rotor designs	3
2.3	Definition of saliency	5
2.4	The Boel Motor	5
3	Theory	7
3.1	Introduction	7
3.2	Transformations	7
3.2.1	Clarke's Transformation	7
3.2.2	Park's Transformation	8
3.3	Motor Equations in the Rotor Reference Frame	9
3.3.1	The Permanent Magnet Synchronous Machine Equivalent Circuits and Mechanical Motor Model	11
4	Control methods	12
4.1	Introduction	12
4.2	Scalar Control	12
4.3	Vector Control	13
4.3.1	Field Oriented Control (FOC)	13
4.3.2	Direct Torque Control (DTC)	16
4.3.3	Voltage Source Inverter	20
5	Field oriented control of different rotor geometries	22
5.1	Introduction	22
5.2	Non Salient Pole Machines (SPMSM)	22
5.3	Negative Salient Pole Machines (NSPMSM)	23
5.4	Positive Salient Pole Machines (PSPMSM)	25

6 Simulink models	27
6.1 Introduction	27
6.2 Existing Simulink Control	27
6.3 Field Oriented Control	29
6.4 Direct Torque Control	29
7 Simulation and results	31
7.1 Field Oriented Control	31
7.2 Direct Torque Control	33
7.3 Comparison of FOC and DTC	35
8 Conclusion	38
8.1 Future work	38
A Derivations	40
A.1 Normalization of negative saliency motor	40
A.2 Normalization of positive saliency motor	42
A.3 Polar coordinates	43
B Simulink model	45
B.1 Field Oriented Control Schematics	45
B.2 Direct Torque Control Schematics	48
B.2.1 Matlab code for Sector calculation	51
B.2.2 Matlab code for Vector selection	51

List of Figures

2.1	Different types of rotor configuration [1]	4
2.2	Two pole permanent magnet rotor	6
3.1	Clarke and Park transform	8
3.2	Salient pole machine equivalent circuit	11
4.1	Overview of available control strategies	12
4.2	Rectangular and polar coordinates	15
4.3	Basic DTC control layout	17
4.4	Hysteresis comparators	19
4.5	Sector division	19
4.6	Output stage of a two level three phase voltage source inverter with an ideal three phase motor model connected	21
5.1	Constant torque loci and current trajectory for MTPA	23
5.2	Direct- and quadrature-axis currents reference	24
5.3	Constant torque loci and current trajectory for MTPA	25
5.4	Direct- and quadrature-axis currents reference	26
6.1	Current calculation of the existing Simulink model	28
6.2	Difference between analytical and Simulink model direct- and quadrature-axis currents	29
7.1	Simulation of FOC with a $15Nm$ load	32
7.2	Measured and Reference currents	33
7.3	Hysteresis control with sample time of $20\mu s$	34
7.4	Hysteresis control with sample time of $2\mu s$	34
7.5	Comparison between measured and estimated sector	35
7.6	Comparison between speed response for FOC and DTC	35
7.7	Comparison between torque response for FOC and DTC	36
7.8	FOC phase currents	36
7.9	DTC phase currents	36
7.10	FOC dq currents	37
7.11	DTC dq currents	37

B.1	Main controller	45
B.2	Current controller / VECT controller	46
B.3	Torque to currents	46
B.4	Torque to quadrature axis current	46
B.5	Torque to direct axis current	46
B.6	Direct- and Quadrature-axis currents to ABC currents	47
B.7	Current regulator	47
B.8	Pulse generator	47
B.9	Main controller	48
B.10	Clarke current transformation	48
B.11	Flux estimator	48
B.12	Two level inverter	49
B.13	Pulse generator	49
B.14	Torque calculator	49
B.15	Torque hysteresis comparator	50
B.16	Voltage estimator, without losses in inverter switches	50

Chapter 1

Introduction

1.1 Introduction

Permanent Magnet Synchronous Motors (PMSM) have long been used in servo motor drives and has lately become more popular in larger motors for industrial applications. Another target application for PMSM is electric vehicles, where its small size and robustness is a big advantage compared to Induction or DC motors. This development of PMSM has been made possible according to the introduction of new magnetic materials like Neodymium Iron Boron ($\text{Nd}_2\text{Fe}_{14}\text{B}$) and Samarium Cobalt (SmCo_5). These types of magnets have a high energy density and high resistance for demagnetization. Previously Ferrite or Aluminium Nickel Cobalt (AlNiCo) magnet had to be used, this made the motors bulky and they were susceptible to demagnetization if the control of the motor current was incorrect. The demagnetization problem was one of the reasons that the $i_d = 0$ control strategy was adopted [2], this works well for round rotors but for a salient rotor a couple of their advantages are lost. It limits the motors speed range and the maximum efficiency cannot be reached. To take advantage of the properties of modern magnetic materials, a new approach to controlling the motors has got possible them has to be taken.

The preferred method for controlling a PMSM is vector control, it can be divided into two main types, Field Oriented Control (FOC) and Direct Torque Control (DTC) and their different subcategories. The FOC aims to control the current vector and DTC aims to control the torque producing flux vector.

1.2 Motivation

The researchers at the Department of Electricity at Uppsala University has recently entered the field of electric motor design, however no real knowledge of motor control of salient pole motors exists in the department. Their high

efficiency motor is designed for battery powered vehicle propulsion system, the efficiency is therefore very important parameter for achieving maximum range. The motor has a few percent advantage compared to conventional multi pole vehicle propulsion motors used today, to utilize this as good as possible the motor should be controlled in the most efficient way.

1.3 Purpose

The purpose of this thesis is to investigate the types of control that is suitable for salient pole permanent magnet synchronous motors, this has been accomplished by doing a literature review over existing control strategies and by implementing some of them in the simulation tool Simulink.

An existing Simulink example model is also examined to find out what type of control is used, to verify its behaviour and to see if it is possible to use it with another motor model with an inverted saliency.

1.4 Thesis Outline

Chapter 2 presents the general theory of Permanent Magnet Synchronous Motors, with focus on different rotor types and their properties, the chapter also present the motor used in this project.

Chapter 3 presents the theory of the PMSM model, and transformation of its parameters into different reference frames.

Chapter 4 gives a presentation of different control methods that can be used for a PMSM.

Chapter 5 presents a more detailed investigation of the preferred control method, Field Oriented Control. It will also present the difference in control strategies for different rotor types.

Chapter 6 presents the existing Field Oriented Control Simulink model, a modified version and a newly developed Direct Torque Control.

Chapter 7 presents the individual simulations and their results of the models from chapter 6, a comparison of the two different types of control are also presented.

Chapter 8 discusses the result of the work and give suggestions for improvements and future work.

Chapter 2

Permanent Magnet Synchronous Motors

2.1 Introduction

The PMSM is a synchronous AC motor, normally with a three phase stator winding similar to induction motors. The rotor however, is different. Permanent magnets provides a constant flux to magnetize the motor. The lack of an electrical magnetization system gives the advantage of a more energy efficient motor.

Depending of the armature winding distribution the PMSM can be divided into two types, BrushLess DC (BLDC) or Permanent Magnet AC (PMAC) motors. The PMAC motor has armature winding that spans close to 180° electrical degrees, which gives the motor a sinusoidal back emf. This is the motor type that this thesis will focus on. The BLDC has armature windings that spans over a smaller angle, which gives the motor a trapezoidal shaped back emf.

The PMSM is normally controlled with a frequency converter that supplies the motor with the correct frequency and voltage/current values.

2.2 Rotor designs

There are many possible design choices for the rotor, some of them can be seen in figure 2.1. Magnets can be mounted on the surface, in the surface and under the surface, all with different advantages/disadvantages. Surface mounted magnets will not withstand high rotational speed due to high centrifugal forces which crack or separates the magnets from the rotor. Subsurface- or buried- magnets need to be insulated from each other with slots or non magnetic material to avoid a magnetic short circuit, but the magnets are protected and held into place at high speeds. Figure 2.1a, 2.1b, 2.1e, 2.1f & 2.1i show rotors with buried magnets.

Figure 2.1a and 2.1f show rotors with damper windings, the winding provides a possibility for asynchronous starting and dampens oscillations.

Figure 2.1g and 2.1h show rotors with rounded magnets, which gives a more sinusoidal field distribution with less harmonics [3].

A rotor with surface magnets has a wide magnetic air gap, resulting in a low magnetizing inductance and difficulty to affect the machines electromagnetic properties by controlling the stator current. With buried magnets the air gap can be smaller and the magnetizing inductance higher, increasing the controllability of the magnetic properties caused by the stator current. This gives the motor a possibility to extend its speed range by reducing the flux, so called flux weakening operation.

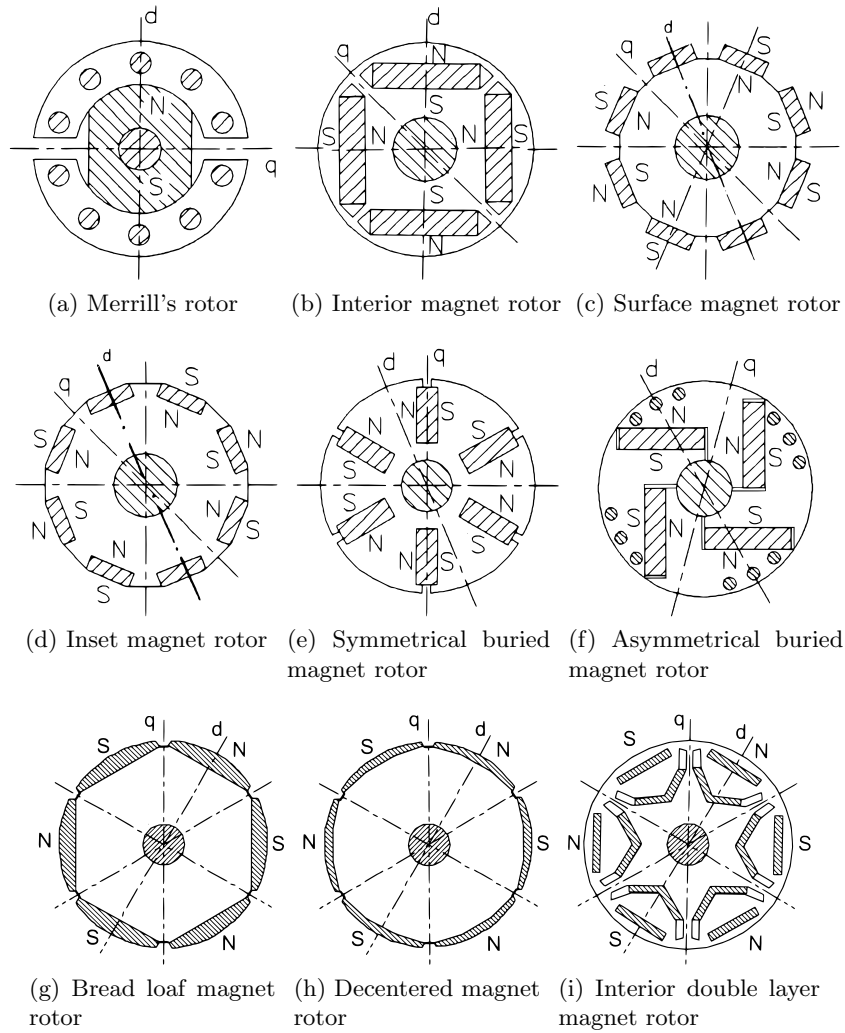


Figure 2.1: Different types of rotor configuration [1]

2.3 Definition of saliency

Saliency is a measure of the non-symmetry of the motors magnetic properties. The non-symmetry occur by the difference in the reluctance path between the rotor and stator. This difference comes from variations of the rotors geometry or material, and a difference can be seen in the motors induction parameters L_d and L_q . Three different types of saliencies can exist, non-, positive- or negative-salient.

It doesn't seem to be any consensus about naming different saliency rotor types, does NS stands for Normal Saliency or Negative Saliency? And what does Normal, Negative, Positive and Inverse means in terms of saliency? Some thinks Inverse Saliency is the opposite compared with a traditional buried magnet rotor ($L_d < L_q$), while other think that Inverse Saliency is the opposite of an electrically excited synchronous rotor ($L_d > L_q$).

To complicate things further a round rotor with magnets attached to the surface will physically look as if it would be salient (see fig. 2.1c), but it doesn't have any saliency at all because the magnets permeability is almost the same as air and will not affect the reluctance path.

Table 2.1: Different conventions of naming of salient machines

	$L_d > L_q$	$L_d < L_q$
Bianchi[4]	Normal	Inverse
Mancado[5]	Inverse	Normal
Mancado[6]	Negative	Positive
Kronberg	Positive	Negative

The author's definition of saliency is based on the traditional electrically excited synchronous machine and its magnetic properties, this will be referred as Positive Saliency.

- SPMSM - Surface mounted Permanent Magnet Synchronous Motor.
Rotor type without any saliency, equal reluctance along the rotor circumference.
- NSPMSM - Negative Saliency Permanent Magnet Synchronous Motor.
Rotor type with lower reluctance between the poles.
- PSPMSM - Positive Saliency Permanent Magnet Synchronous Motor.
Rotor type with lower reluctance at the poles.

2.4 The Boel Motor

The control methods discussed in this thesis is intended for use with a high speed, high efficiency motor developed at Uppsala University. The motor

is designed for use with a 2:1 differential gear or direct drive with small vehicular wheel in mind.

The development of electric propulsion systems by car manufacturers has mostly been focused on four, six or eight pole motor with a poor efficiency below 95%. However, with the solution of Maxwell's equations it is realized that for high speed drives, the smaller amount of poles the more compact and cost effective the motor will be. Simulations show an efficiency between 95-98% through the operating range. [7]

The motor is said to be a downscaled version of a 1.6 GW nuclear turbo generator with a permanent magnet rotor and cable windings. The rotor is of simple construction with a permanent magnet sandwiched between the two iron poles bolted together with the rotor end plates (figure 2.2).



Figure 2.2: Two pole permanent magnet rotor

Cable windings gives a uniform electrical field, which utilizes the insulation material as good as possible, compared to square windings which have higher electrical stress in the corners. The use of cables gives the possibility to use higher voltage and lower currents for the same power, thus reducing copper losses in the windings.[8]

The motors most important parameters from a control perspective can be seen in table 2.2.

Table 2.2: Motor parameters

$V_{rated,LL,rms}$	260V	R_s	0.015Ω	p	2
ϕ	3	L_d	4mH	rpm	0 – 3000
$I_{rated,rms}$	49A	L_q	1mH	J_{est}	0.003334kgm ²
I_{max}	100A	$\lambda_{pm,fullload}$	0.1960Wb	F_{est}	0.00425Nm
P_{rated}	30kW				
P_{max}	60kW				

Chapter 3

Theory

3.1 Introduction

A three phase PMSM is normally constructed with sinusoidally distributed phase windings, with a 120° phase shift between the three windings. In a stator reference frame coordinate system the phase vectors A, B, C can be seen as they are fixed in angle, but with time varying amplitudes. This three vector representation makes calculation of machine parameters unnecessarily complex. By transforming the system into a two vector orthogonal system, the necessary calculations could be much simpler.

3.2 Transformations

A three phase machine can be described by a set of differential equations with time dependent coefficients. By transforming the motor parameters, the complexity of machine calculations can be reduced. The most common methods to do this are the Clarke and Park transformations.

According to the definitions the transforms give a third component, 0 or zero-sequence. But since a motor normally is a balanced load, the zero-sequence can be ignored.

The two transformations presented below are not the original Clarke and Park, but in a slightly modified form to make them power invariant [9]. By using these modifications it is possible to calculate the correct power/-torque values from the transformed motor parameters without the need to transform them back to three phase values.

3.2.1 Clarke's Transformation

The Clarke transformation changes a three phase system into at two phase system with orthogonal axes in the same stationary reference frame. The new two phase variables are denoted α and β , the original and transformed

system can be seen in figure 3.1a. The ABC parameters are transformed into $\alpha\beta 0$ parameters by equation (3.1), and in reverse by equation (3.2) [10].

$$f_{\alpha\beta 0} = T f_{ABC} \quad (3.1)$$

$$f_{ABC} = T^{-1} f_{\alpha\beta 0} \quad (3.2)$$

Where f can be any one of the motors armature parameters, and the transformation matrix T is.

$$T = \sqrt{\frac{2}{3}} \begin{bmatrix} 1 & -\frac{1}{2} & -\frac{1}{2} \\ 0 & \frac{\sqrt{3}}{2} & -\frac{\sqrt{3}}{2} \\ \frac{1}{\sqrt{2}} & \frac{1}{\sqrt{2}} & \frac{1}{\sqrt{2}} \end{bmatrix} \quad (3.3)$$

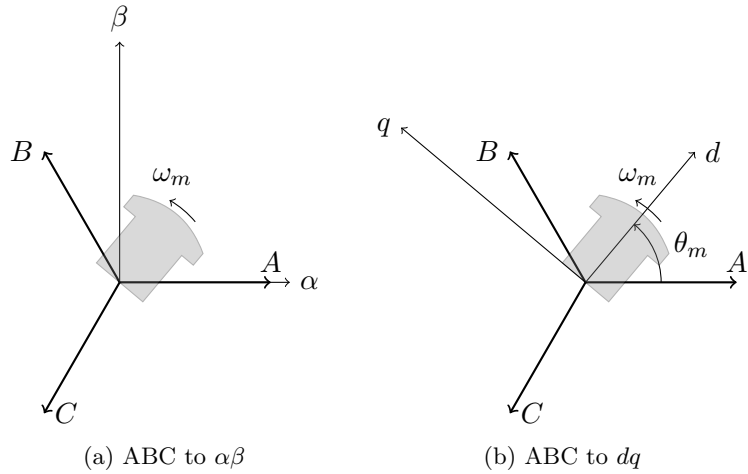


Figure 3.1: Clarke and Park transform

3.2.2 Park's Transformation

The Park transformation changes a three phase system in one stationary reference frame into a two phase system with orthogonal axes in a different rotating reference frame. The two new phase variables are denoted d and q , and are referred to as the motors direct- and quadrature-axis. The original and transformed system can be seen in figure 3.1b. The ABC parameters are transformed into $dq0$ parameters by equation (3.4), and in reverse by equation (3.5) [10].

$$f_{dq0} = T(\theta) f_{ABC} \quad (3.4)$$

$$f_{ABC} = T(\theta)^{-1} f_{dq0} \quad (3.5)$$

Where f can be any one of the motors armature parameters, and the transformation matrix T is.

$$T = \sqrt{\frac{2}{3}} \begin{bmatrix} \cos(\theta_m) & \cos(\theta_m - \frac{2\pi}{3}) & \cos(\theta_m + \frac{2\pi}{3}) \\ \sin(\theta_m) & \sin(\theta_m - \frac{2\pi}{3}) & \sin(\theta_m + \frac{2\pi}{3}) \\ \frac{1}{\sqrt{2}} & \frac{1}{\sqrt{2}} & \frac{1}{\sqrt{2}} \end{bmatrix} \quad (3.6)$$

By using the Park's transform, the stator parameters such as voltages, currents, and flux linkages, are associated with fictitious stator windings that rotate with the rotor. The time varying parameters between stator and rotor are thus eliminated and all variables are expressed in the same orthogonal or mutually decoupled direct- and quadrature-axes.

3.3 Motor Equations in the Rotor Reference Frame

After the described transformation the different parameters in a synchronous machine can be described by the following equations.[1].

$$v_{sd} = R_s i_{sd} + \frac{d\lambda_{sd}}{dt} - \omega_e \lambda_{sq} \quad (3.7)$$

$$v_{sq} = R_s i_{sq} + \frac{d\lambda_{sq}}{dt} + \omega_e \lambda_{sd} \quad (3.8)$$

$$v_D = R_D i_D + \frac{d\lambda_D}{dt} = 0 \quad (3.9)$$

$$v_Q = R_Q i_Q + \frac{d\lambda_Q}{dt} = 0 \quad (3.10)$$

The flux linkages above are defined as:

$$\lambda_{sd} = (L_{md} + L_{s\sigma}) + L_{md} i_D + \lambda_{pm} = L_{sd} i_{sd} + L_{md} i_D + \lambda_{pm} \quad (3.11)$$

$$\lambda_{sq} = (L_{mq} + L_{s\sigma}) + L_{mq} i_Q = L_{sq} i_{sq} + L_{mq} i_Q \quad (3.12)$$

$$\lambda_D = L_{md} i_{sd} + L_D i_D + \lambda_{pm} \quad (3.13)$$

$$\lambda_Q = L_{mq} i_{sq} + L_Q i_Q \quad (3.14)$$

By describing the Permanent Magnet as a current source, the flux linkage λ_{pm} can be seen as.

$$\lambda_{pm} = L_{md} i_{pm} \quad (3.15)$$

The subscripts d and q denotes if the component is along the direct- or quadrature-axes, and:

v_{sd} and v_{sq} are the terminal voltage components.

v_D and v_Q are the induced voltage in the damper windings and can be considered to be zero at steady state.

i_{sd} and i_{sq} are the armature winding current components.

L_{sd} and L_{sq} are the armature self inductances components.

$L_{s\sigma}$ is the stator leakage inductance.

R_s is the armature winding resistance.

λ_{pm} is the flux linkage per phase generated from the excitation system.

R_D and R_Q are the damper windings resistance.

L_D and L_Q are the damper windings self inductance.

Instantaneous power in abc reference system is defined as.

$$P_{in,abc} = v_a i_a + v_b i_b + v_c i_c \quad (3.16)$$

Using the above transformation it is expressed in dq0 domain as.

$$P_{in,dq} = \frac{3}{2} v_d i_d + \frac{3}{2} v_q i_q + 3 v_0 i_0 \quad (3.17)$$

Ignoring zero sequence and inserting (3.7) and (3.8) into the above.

$$P_{in,dq} = \omega_e \frac{3}{2} (\lambda_d i_{sq} - \lambda_q i_{sd}) + \frac{3}{2} \left(R_s i_{sd}^2 + \frac{d\lambda_{sd}}{dt} i_{sd} + R_s i_{sq}^2 + \frac{d\lambda_{sq}}{dt} i_{sq} \right) \quad (3.18)$$

Where the first term accounts for the electromagnetic power and ω_e is the electrical angular frequency. The mechanical angular frequency can be expressed as: $\omega_e = \frac{p}{2}\omega_m$, where p is the number of poles. Assuming steady state, the electromagnetic power P_e can be expressed as.

$$P_e = \omega_m \frac{3}{2} \frac{p}{2} (\lambda_{sd} i_{sq} - \lambda_{sq} i_{sd}) \quad (3.19)$$

Divide the power with rotational speed ω_m to get the motors electromechanical torque T_e and replace the flux linkages λ_{sd} and λ_{sq} with equations (3.11) and (3.12).

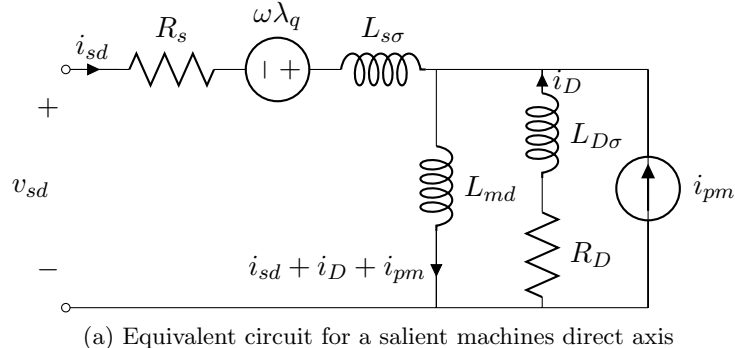
$$T_e = \frac{3}{2} \frac{p}{2} [(L_d i_{sd} + \lambda_{pm}) i_{sq} - L_{sq} i_{sq} i_{sd}] \quad (3.20)$$

For a rotor with damper windings the torque equation is expressed as equation 3.21, this thesis focuses on control of machines without damper windings an in steady state, i.e. the terms for damper windings are here ignored.

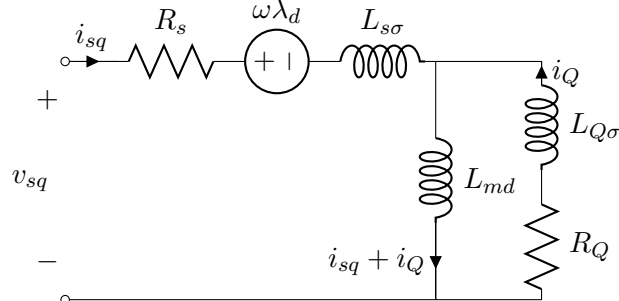
$$T_e = \frac{3}{2} \frac{p}{2} [\lambda_{pm} i_{sq} + (L_{md} - L_{mq}) i_{sd} i_{sq} + L_{md} i_D i_{sq} + L_{mq} i_Q i_{sd}] \quad (3.21)$$

3.3.1 The Permanent Magnet Synchronous Machine Equivalent Circuits and Mechanical Motor Model

To be able to simulate the electrical behaviour of the motor in any electrical circuit analysis program the motors equivalent circuit (figure 3.2) is needed. By transforming the drive voltage into dq parameters and connecting it to its respective dq equivalent circuit, measurement of the models currents can be done. From the current values the motors torque can be calculated and



(a) Equivalent circuit for a salient machines direct axis



(b) Equivalent circuit for a salient machines quadrature axis

Figure 3.2: Salient pole machine equivalent circuit

the speed can be calculated from.

$$\frac{p}{2} (T_e - T_L) = J \frac{d\omega_r}{dt} \quad (3.22)$$

Where T_L is the load torque, ω_r is the rotational speed and J is the motor and loads inertia.

With the above parameters it is possible to implement a model of a PMSM in a circuit simulation software. However, in this thesis the existing Simulink model has been used.

Chapter 4

Control methods

4.1 Introduction

Synchronous motors have to be driven by a Variable Frequency Drive (VFD) to be able to run at different speeds. Control methods for electric motors can be divided into two main categories depending of what quantities they control. The control algorithm Scalar Control controls only magnitudes, whereas the algorithms Vector Control controls both magnitude and angles. These two main methods can be further divided into a number of different methods depending of their functionality, an overview over different control methods can be seen in figure 4.1.

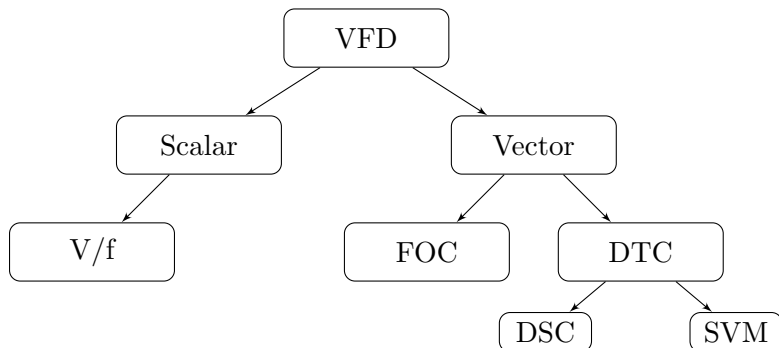


Figure 4.1: Overview of available control strategies

4.2 Scalar Control

The simplest method to control a PMSM is scalar control, where the relationship between voltage or current and frequency are kept constant through the motors speed range. The frequency is set according to the wanted synchronous speed and the magnitude of the voltage/current is adjusted to keep

the ratio between them constant. No control over angles is utilized, hence the name scalar control. The method uses an open-loop control approach without any feedback of motor parameters or its position. This makes the method easy to implement and with low demands on computation power of the control hardware, but its simplicity also comes with some disadvantages. One of them are instability of the drive system after exceeding a certain applied frequency, to overcome this the rotor has to be constructed with damper windings to assure synchronization of the rotor to the electrical frequency [11]. This will limit the number of design choices for the rotor, e.g. the magnets has to be located on the inside of the damper bars. Most PMSM are therefore constructed without damper windings, and they are not suitable for traditional scalar control. Another drawback with the lack of feedback is the systems low dynamic performance, which limits the use of this control method to e.g. fan- and pump-drives [11]. For applications that demands high dynamic performance, vector control is recommended. One way to improve the performance without the use of position feedback is to use the variations in the inverters DC link voltage to determine the correct modulation [12] [13].

4.3 Vector Control

With control of both magnitude and the angle of the flux it is possible to achieve higher dynamic performance of the drive system than scalar control can offer. Two different types of strategies exist for vector control, Field Oriented Control and Direct Torque Control.

4.3.1 Field Oriented Control (FOC)

In Field Oriented Control the goal is to control the direct- and quadrature-axis current i_d and i_q to achieve the requested torque, equation (3.20) shows the torque as a function of the current components. By controlling i_d and i_q independently it's possible to achieve a Maximum Torque Per Ampere ratio (MPTA) to minimize the current needed for a specific torque, which maximizes the motors efficiency.

For a non-salient machine i.e. $L_d = L_q$, the control is easy to implement. From equation (3.20) it can be seen that a motor without saliency cannot produce any reluctance torque. i_d has therefore no effect on torque production, and it needs to be zero at all times to reach MPTA. The torque curves will be linear in the dq-plane and the MPTA trajectory will be along the quadrature-axis.

For a salient machine, i.e. $L_d \neq L_q$ the control is a bit more difficult to implement since the motor produces both electromechanical and reluctance torque, see to equation (3.20). That's why the torque as a function of current

in the dq-plane is no longer linear. To reach MPTA, the minimum distance from the origin to the curve of requested torque has to be calculated.

A number of different methods for calculating the optimal currents are mentioned in the literature, for example in [2], [14], and [15] further described below.

One of the critical parameters for FOC the need of correct information of the motors position. The most common way to do this is Indirect FOC (IFO), where a mechanical sensor coupled to the motors shaft is used for positioning. Another type is Direct FOC (DFO) where the position is estimated from the flux- or back EMF vector [15].

Other critical parameters are the varying values of inductances L_d and L_q as they constantly changing during different operating conditions due to saturation etc. The direct axis inductance is more affected, which gives the motor a higher saliency ratio.

Normalization of Variables

This method was introduced by Jahns et al.[14] in 1986 as a method for stator current vector control. The article describes how to normalize the parameters and express the torque equation in a p.u.-system, with the motor parameters eliminated from the equation. The normalized torque is then expressed as.

$$T_{en} = i_{qn}(1 - i_{dn}) \quad (4.1)$$

The total current i_n can be expressed as the modulus of i_{dn} and i_{qn}

$$i_n = \sqrt{i_{dn}^2 + i_{qn}^2} = 1 \quad (4.2)$$

By combine (4.1) and (4.2), differentiate the expression with respect to i_{dn} and i_{qn} , setting the results to zero and solving the two expressions for T_{en} . The torque can then be expressed as a function of either i_{dn} or i_{qn} .

$$T_{en}^* = \sqrt{i_{dn}^*(i_{dn}^* - 1)^3} \quad (4.3)$$

$$T_{en}^* = \frac{i_{qn}^*}{2} \left(1 + \sqrt{1 + 4(i_{qn}^*)^2} \right) \quad (4.4)$$

A derivation of the equation used in this method can be seen in appendix A.1.

Polar Coordinates

Another method for calculating the optimal current trajectory is to transform the torque equation in the dq reference frame into polar coordinates [2]. By substituting i_d and i_q with its corresponding expressions in polar coordinates illustrated in figure 4.2 a new equation for the torque is obtained.

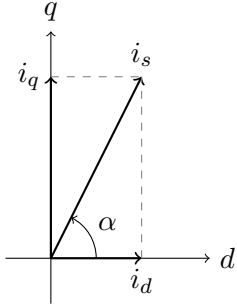


Figure 4.2: Rectangular and polar coordinates

$$i_d = i_s \cos(\alpha) \quad (4.5)$$

$$i_q = i_s \sin(\alpha) \quad (4.6)$$

$$\alpha = \arctan\left(\frac{i_q}{i_d}\right) \quad (4.7)$$

The torque equation can then be expressed as a function of the stator current i_s and the current vector angle α .

$$T_e = \frac{3}{2} \frac{p}{2} \left[\lambda_{pm} i_s \sin(\alpha) + (L_d - L_q) i_s^2 \frac{1}{2} \sin(2\alpha) \right] \quad (4.8)$$

By differentiating equation (4.8) with respect to α , setting the result to zero and reverse substitute the variables, following expression is given.

$$\lambda_{pm} i_d + (L_d - L_q) i_d^2 - (L_d - L_q) i_q^2 = 0 \quad (4.9)$$

From equation (4.9) the direct-axis current can be expressed as a function of stator current magnitude $|i_s|$

$$i_d^* = \frac{\lambda_m}{4(L_d - L_q)} - \sqrt{\frac{\lambda_m^2}{16(L_d - L_q)^2} + \frac{|i_s^*|^2}{2}} \quad (4.10)$$

And the quadrature-axis current can be solved from the current modulus equation.

$$i_q^* = \sqrt{|i_s^*|^2 - i_d^{*2}} \quad (4.11)$$

Saliency Ratio

A third method for calculating the optimal current trajectory is presented in Advanced Electrical Drives: Analysis, Modelling, Control [15]. By normalizing the variables, introducing the saliency ratio χ and short circuit ratio κ , the torque equation can be expressed as.

$$T_e^n = i_{sq}^n \left(1 - \frac{2\chi}{\kappa} i_{sd^n} \right) \quad (4.12)$$

Where.

$$i_s^{sc} = \frac{\lambda_{pm}}{\sqrt{L_{sd}^2 + L_{sq}^2}} \quad (4.13)$$

$$i_{sd}^n = \frac{i_{sd}}{i_s^{max}} \quad (4.14)$$

$$i_{sq}^n = \frac{i_{sq}}{i_s^{max}} \quad (4.15)$$

$$\kappa = \frac{i_s^{sc}}{i_s^{max}} \quad (4.16)$$

$$\chi = \frac{L_{sq} - L_{sd}}{2L_{sd}} \quad (4.17)$$

The term i_s^{max} represents the maximal stator current. The normalized direct- and quadrature currents are then expressed as.

$$i_{sd}^n = \frac{\kappa}{8\chi} - \sqrt{\frac{(i_s^n)^2}{2} + \left(\frac{\kappa}{8\chi}\right)^2} \quad (4.18)$$

$$i_{sq}^n = \sqrt{(i_s^n)^2 - (i_{sd}^n)^2} \quad (4.19)$$

4.3.2 Direct Torque Control (DTC)

Direct Torque Control was first introduced for induction motors (IM) by Takahashi and Noguchi [16] in 1984 and the Direct Self Control method by Depenbrock [17] in 1985. The methods were characterized by their simplicity, good performance and robustness. Unlike the FOC method, DTC worked without any external measurement of the rotors mechanical position. However, to ensure correct rotational direction of a PMSM, the rotor position shall be known at motor start up. The reason behind the simplicity is that DTC not require any current regulators, transformations to rotating reference frame or PWM generators.

The disadvantages are, difficulty to control torque at low speed, high current and torque ripple, variable switching frequency, high noise level at low speed and lack of direct current control. It is also important to do a correct estimation of the dc-link voltage and stator resistance to get stability of the drive system [18].

There are a number off different suggestions for improving the characteristics of DTC, such as.

- Improved switching tables and increasing the number of sectors [19] [20].
- Using multilevel hysteresis comparators [20].

- Fixed frequency switching with PWM or Space Vector Modulation (SVM) [20] [21]

The working principle for the basic DTC is to select a voltage vector based on the error between requested and actual values of torque and flux linkage, it also uses a rough position estimation that divides one electrical revolution into six sectors depending on the flux linkage angle. A basic scheme for DTC can be seen in figure 4.3, the different blocks are described below [22].

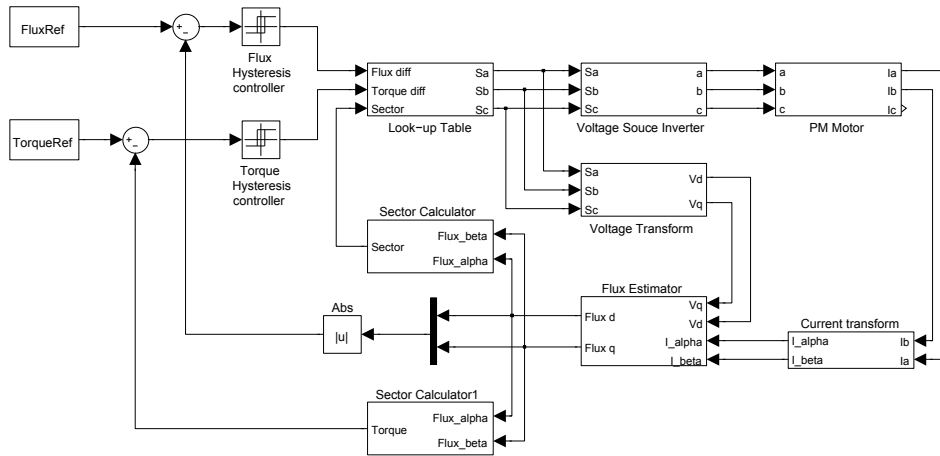


Figure 4.3: Basic DTC control layout

Current Transform

The measured motor currents are calculated with the Clarke transform from ABC phase reference frame into the $\alpha\beta$ reference frame, as described in section 3.2.1

Voltage Transform

The voltage u_{est} is estimated from the inverters switching state and the DC-link voltage in the $\alpha\beta$ reference frame by the voltage equation [18] [22].

$$u_{est}(S_{ABC}) = \sqrt{\frac{2}{3}} \frac{U_{dc}}{2} \left(S_A e^{j0} + S_B e^{j\frac{2\pi}{3}} + S_C e^{j\frac{4\pi}{3}} \right) - \sqrt{\frac{2}{3}} \left(u_A e^{j0} + u_B e^{j\frac{2\pi}{3}} + u_C e^{j\frac{4\pi}{3}} \right) \quad (4.20)$$

Where u_{ABC} is the voltage loss in the power switches and S_{ABC} is the state of the power switches, further described under **Voltage Source Inverter** on page 20.

Flux Estimator

From the transformed voltages and currents it's possible to estimate the stator flux $\lambda_{\alpha\beta,est}$, see equation (4.21).

$$\lambda_{\alpha\beta,est} = \int (v_{\alpha\beta} - R_s i_{\alpha\beta}) dt \quad (4.21)$$

The magnitude of the estimated flux $\lambda_{\alpha\beta,est}$ is calculated and compared with the requested flux $\lambda_{\alpha\beta}^*$.

Torque Calculation

By divide equation (3.19) with the motors mechanical rotational speed ω_m and replace the variables with the transformed ones, an expression for a flux and current depending torque is acquired.

$$T_{e,est} = \frac{3}{2} \frac{p}{2} (\lambda_{s\alpha} i_{s\beta} - \lambda_{s\beta} i_{s\alpha}) \quad (4.22)$$

The estimated torque $T_{e,est}$ is calculated and compared with the requested torque T_e^* .

Torque and Flux Hysteresis Comparator

To determine the correct control commands one flux and one torque hysteresis comparators are used. The comparators evaluate the difference between requested values and estimated values, and thereby determine if the flux and torque vectors should be:

- Increased - Output is 1
- Decreased - Output is -1
- Constant - Output is 0

The torque comparator works with all three levels, whereas the flux comparator only works with two levels, since the stator flux can't be kept constant during operation of the permanent magnet motor.

Sector Calculation

To determine the motors operating sector, the flux vector angle θ_{λ_s} has to be calculated from the estimated flux with equation (4.23).

$$\tan^{-1}(\theta_{\lambda_s}) = \frac{\lambda_\beta}{\lambda_\alpha} \quad (4.23)$$

Depending on the angle of the flux vector, the correct sector S_{1-6} is chosen, see figure 4.5.

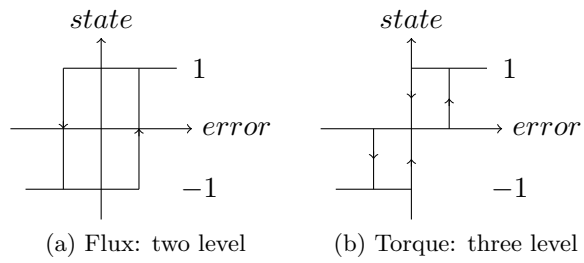


Figure 4.4: Hysteresis comparators

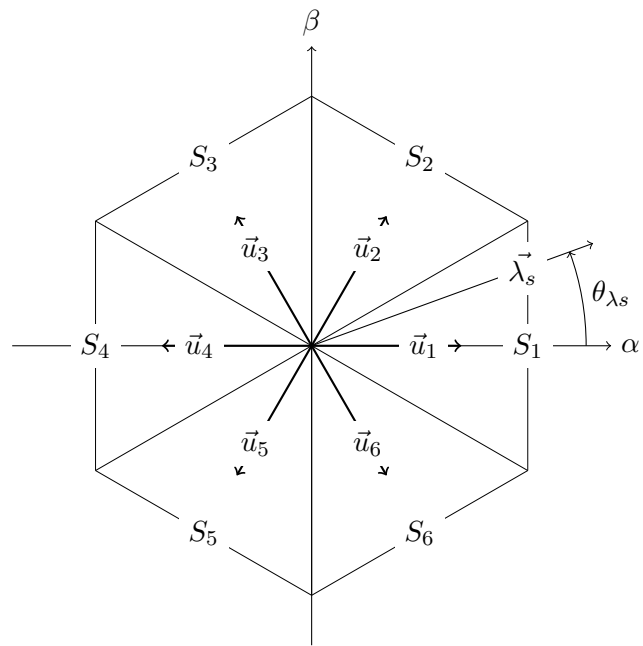


Figure 4.5: Sector division

Look Up Table

The states from the hysteresis comparator ($d\lambda, dT$) are read by the look-up block together with the calculated sector number, and from table 4.1 the correct voltage vector is chosen. Table 4.2 show the corresponding switch

Table 4.1: Basic DTC switching table

		Sector					
		1	2	3	4	5	6
$d\lambda = +1$	$dT = +1$	\vec{u}_2	\vec{u}_3	\vec{u}_4	\vec{u}_5	\vec{u}_6	\vec{u}_1
	$dT = 0$	\vec{u}_0	\vec{u}_7	\vec{u}_0	\vec{u}_7	\vec{u}_0	\vec{u}_7
	$dT = -1$	\vec{u}_6	\vec{u}_1	\vec{u}_2	\vec{u}_3	\vec{u}_4	\vec{u}_5
$d\lambda = -1$	$dT = +1$	\vec{u}_3	\vec{u}_4	\vec{u}_5	\vec{u}_6	\vec{u}_1	\vec{u}_2
	$dT = 0$	\vec{u}_7	\vec{u}_0	\vec{u}_7	\vec{u}_0	\vec{u}_7	\vec{u}_0
	$dT = -1$	\vec{u}_5	\vec{u}_6	\vec{u}_1	\vec{u}_2	\vec{u}_3	\vec{u}_4

position for the inverter to achieve the selected voltage vector.

Table 4.2: Switch positions and their corresponding voltage vector

	S_A	S_B	S_C		S_A	S_B	S_C
\vec{u}_1	1	0	0	\vec{u}_4	0	1	1
\vec{u}_2	1	1	0	\vec{u}_5	0	0	1
\vec{u}_3	0	1	0	\vec{u}_6	1	0	1
\vec{u}_0	0	0	0	\vec{u}_7	1	1	1

4.3.3 Voltage Source Inverter

Both FOC and DTC strategies require an inverter to convert the low voltage control signals to high voltage to drive the motor. The inverter is connected to the motor terminals as seen in figure 4.6 and is controlled by three signal $S_{A,B,C}$. Each signal controls both high $_h$ and low $_l$ side switches of the corresponding phase. When signal S_A is high, switch A_h is turned on while switch A_l turned off. When signal S_A is low, switch A_h is turned off while switch A_l turned on. Same method is applied for the other two phases B and C .

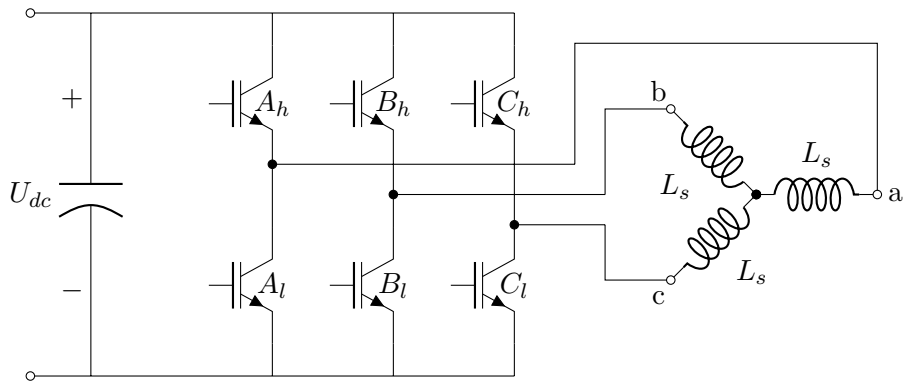


Figure 4.6: Output stage of a two level three phase voltage source inverter with an ideal three phase motor model connected

In this thesis the FOC inverter is controlled by a hysteresis controller, but it could also be done by using for example SPWM or SVPWM modulation. The DTC controls the inverter from the look up block using table 4.1 and 4.2.

Chapter 5

Field oriented control of different rotor geometries

5.1 Introduction

Depending of the different rotor geometries discussed in chapter 2, the current control strategies differs. The non salient type has a linear current trajectory, while the salient ones have a curved current trajectory. The main difference between positive and negative saliency is that the direct axis current is mirrored over the quadrature axis because of the inversion of L_d and L_q .

5.2 Non Salient Pole Machines (SPMSM)

For a non-salient pole machine the direct- and quadrature-axes inductances are equal, assuming steady state operation. The torque equation (3.20) can hence be simplified to (5.1).

$$T_e = \frac{3}{2} \frac{P}{2} [\lambda_{pm} I_{sq}] \quad (5.1)$$

From (5.1) it can be seen that the only torque producing current is along the quadrature-axis. To reach maximum efficiency of the machine, you would like maximize the torque per ampere relationship (MPTA). This is easily achieved by keeping the direct-axis current to zero at all times. The control systems reference currents i_q^* and i_d^* can easily be calculated from (5.2) and (5.3).

$$i_q^* = \frac{T_e^*}{\frac{3}{2} \frac{P}{2} \lambda_{pm}} \quad (5.2)$$

$$i_d^* = 0 \quad (5.3)$$

5.3 Negative Salient Pole Machines (NSPMSM)

For a salient pole machine the direct- and quadrature-axes inductances are unequal, the most common type is the NSPMSM where $L_d < L_q$. Assuming steady state operation, the torque equation(3.21) simplifies to.

$$T_e = \frac{3}{2} \frac{P}{2} [\lambda_{pm} I_{sq} - (L_q - L_d) I_{sd} I_{sq}] \quad (5.4)$$

From (5.4) it can be seen that there are two terms affecting the torque production, the electromechanical torque $\frac{3}{2} \frac{P}{2} \lambda_{pm} I_{sq}$ and the reluctance torque $\frac{3}{2} \frac{P}{2} (L_d - L_q) I_{sd} I_{sq}$.

To visualize the current control strategy, the normalization method mentioned in chapter 4.3.1 is used. Rearranging (4.1) to.

$$i_{qn} = \frac{T_{en}}{1 - i_{dn}} \quad (5.5)$$

From equation (5.5) the constant torque loci can be plotted in the dq-plane. By setting (4.3) and (4.3) equal and solving it for direct axis current, an equation for the MPTA curve is obtained.

$$i_{dn}^* = \frac{1}{2} \left(1 - \sqrt{1 + 4(i_{qn}^*)^2} \right) \quad (5.6)$$

Figure 5.1 show the normalized torque loci, MPTA current trajectory and the maximum current circle plotted on the dq plane. The maximum current $i_{s,max}$ is determined either by the inverters output transistors or the stator windings, and in normalized terms the maximum current is always 1.

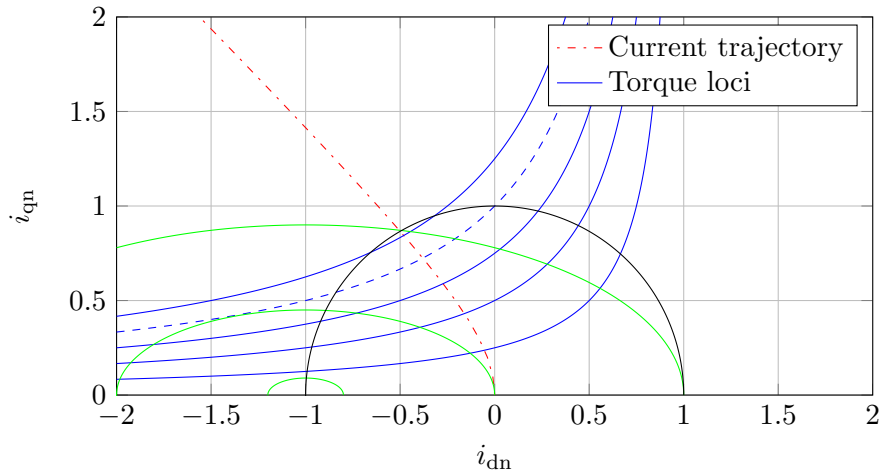


Figure 5.1: Constant torque loci and current trajectory for MTPA

Figure 5.2 shows the individual direct and quadrature axis currents.

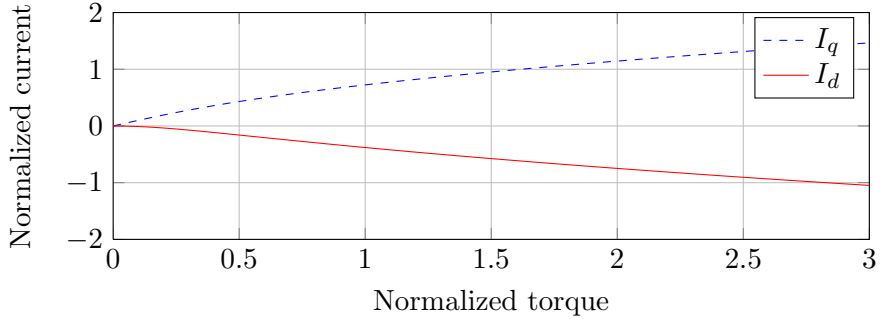


Figure 5.2: Direct- and quadrature-axis currents reference

The maximum voltage $V_{s,max}$ is limited by either the inverters dc-link voltage or the stator windings insulation, this voltage limit will determine the motors base speed. By rearranging the voltage equation (5.7) to equation (5.8).

$$V_s = \omega_s \sqrt{\lambda_d^2 + \lambda_q^2} = \omega_s \sqrt{(\lambda_{pm} + L_{sd}i_{sd})^2 + (L_{sq}i_{sq})^2} \quad (5.7)$$

$$\left(\frac{V_s}{\omega_s}\right)^2 = \frac{(i_{sd} + \lambda_{pm}L_{sq}^{-1})^2}{L_{sd}^{-2}} + \frac{i_{sq}^2}{L_{sq}^{-2}} \quad (5.8)$$

Which describes an ellipse with its centre in $-\lambda_{pm}L_{sq}^{-1}$ and the axes.

$$a = \frac{\frac{V_s}{\omega_s}}{L_{sd}}$$

$$b = \frac{\frac{V_s}{\omega_s}}{L_{sq}}$$

The ellipse defines another current limit. The motors operating point has to be inside both the current circle and the voltage ellipse. As the ellipse shrinks when the speed increases, the previously calculated current references are not valid above base speed. The reason is the generated emf from the motor, as the speed increases the motors induced back emf increases as well. When the back emf exceeds the inverters dc-voltage, it can no longer continue delivering current along the requested trajectory. A different control method has to be implemented to be able to run the motor above base speed without a drastic drop in torque. The common way of doing this on traditional synchronous motors is to reduce the rotors field current, thus reducing the air gap flux. This method is called field weakening. But for a PMSM the magnets can obviously not be controlled, so the air gap flux has to be weakened by other means. The method is called flux weakening and the weakened air gap flux is achieved by decreasing the direct axis current.

5.4 Positive Salient Pole Machines (PSPMSM)

Another type of the salient pole machine is the PSPMSM where $L_d > L_q$, the difference in inductances makes the current reference calculated for the NSPMSM invalid. The torque equation (5.4) is the same, but for the same current reference the motor produces a negative reluctance torque, counter-acting the electromagnetic torque. A solution for this is derived in appendix A.1 with a newly defined base current, the order of L_{md} and L_{mq} is switched to keep the base current positive.

$$i_b = \frac{\lambda_{pm}}{(L_{sd} - L_{sq})} \quad (5.9)$$

This new base current gives after recalculation of the derivation in appendix A.1 a new equation for the electromechanical torque in p.u.

$$T_{en} = i_{qn}(1 + i_{dn}) \quad (5.10)$$

To visualize the torque loci.

$$i_{qn} = \frac{T_{en}}{1 + i_{dn}} \quad (5.11)$$

Figure 5.3 show the normalized torque loci, MPTA current trajectory, maximum current circle and voltage ellipse plotted on the dq plane. Figure 5.4

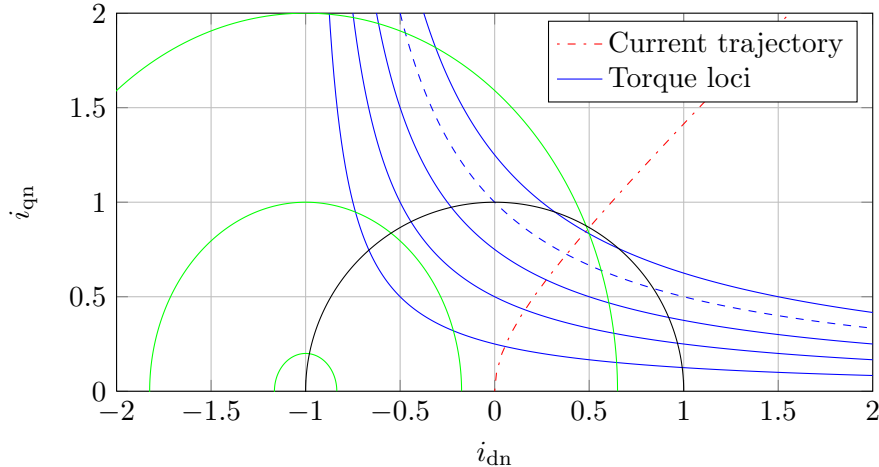


Figure 5.3: Constant torque loci and current trajectory for MTPA

shows the individual direct and quadrature axis currents.

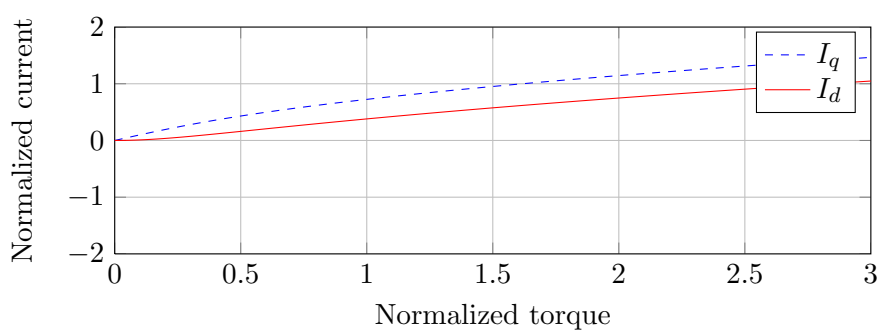


Figure 5.4: Direct- and quadrature-axis currents reference

Chapter 6

Simulink models

6.1 Introduction

All simulations have been implemented in Simulink, the software provides an interactive graphical environment and a customizable set of block libraries that let you design, simulate, implement and test a variety of time-varying systems. This makes it simpler to visualize and rapidly develop a control system unlike traditional C or Matlab-code.

The scalar control was ruled out already in the literature study as a useful candidate for electric vehicles because of its poor performance. The two control methods chosen for simulation are basic version of Field Oriented Control and Direct Torque Control, without any special solutions to get around eventual problems in the methods. This is done mainly to investigate the behaviour of the different methods.

6.2 Existing Simulink Control

One aim of this work was to investigate if the existing "Simulink ac6_IPMSM" example could be used for verifying the behaviour of the motor, the controller consists of two major blocks for speed-/torque- and vector-control. Looking at the vector controller it can be seen that the first part (figure 6.1) outputs the direct- and quadrature-axis current references, the second part generates the pulses to the inverter with a hysteresis controller.

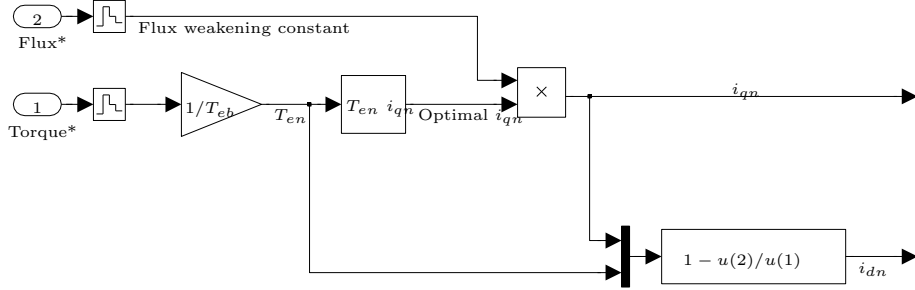


Figure 6.1: Current calculation of the existing Simulink model

Since the controller calculates direct- and quadrature-axis currents references it can be classified as a Field Oriented Control. The equations that govern the behaviour are.

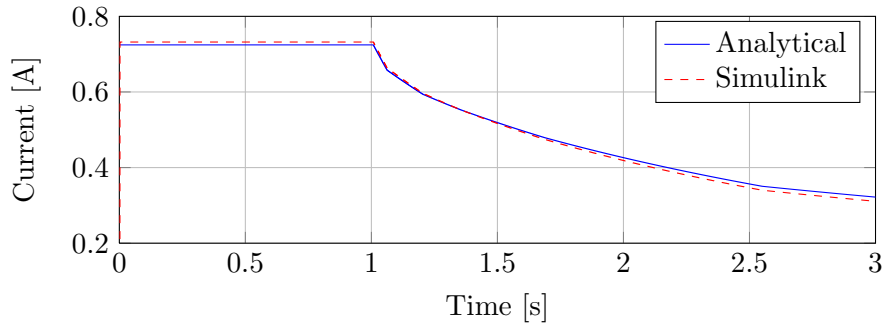
$$T_{en} = \frac{T^*}{T_{eb}} \quad (6.1)$$

$$i_{qn} = \frac{\sqrt{4\frac{1}{2}T_{en} + 1} - 1}{2\frac{1}{2}} \quad (6.2)$$

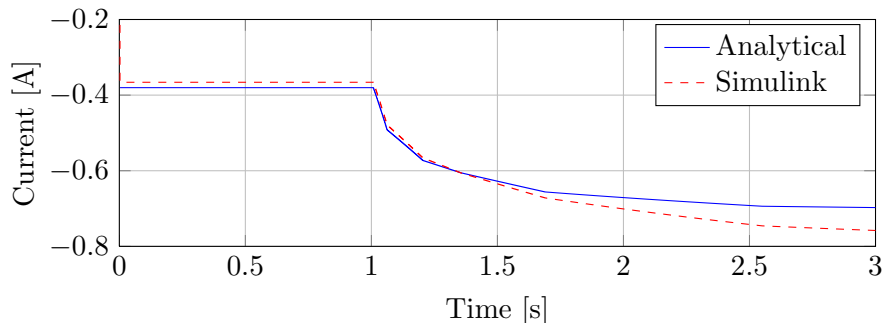
$$i_{dn} = 1 - \frac{T_{en}}{i_{qn}} \quad (6.3)$$

Equation (6.1) and (6.3) are the same as the ones derived in appendix A.5, whereas equation (6.2) differs. Given the complexity of equation (A.17) it can be safe to assume that the Simulink version is an approximated version of the analytically solved one, the difference between them can be seen in the simulation result in figure 6.2. The simulation shows that the different equations gives approximately the same result for normal operation and in the beginning of flux weakening region, far into flux weakening region the difference between direct axis currents increases.

The model implements flux weakening by using a pre calculated values in a look up table, the value is between 1-0 and is used to reduce the quadrature axis current by a certain percentage for the pre calculated operation point.



(a) Quadrature axis currents



(b) Direct axis current

Figure 6.2: Difference between analytical and Simulink model direct- and quadrature-axis currents

6.3 Field Oriented Control

The field oriented control model is based on the existing Simulink model discussed in the previous section and modified with the changes of base current and quadrature axis current calculation proposed in chapter 5.4. The existing speed/torque controller has also been replaced with a PI-regulator with a speed error signal as input and a torque request as output, and the motor parameter (table 2.2) has been changed to conform to the new motor. An overview of the controller and its most important blocks can be seen in appendix B.1

6.4 Direct Torque Control

The direct torque model has been developed to use the same speed control and motor parameters as the field oriented one, an overview of the controller and its most important blocks can be seen in appendix B.2. The two blocks for sector and vector calculation are not built using Simulinks "symbolic programming", but rather in conventional Matlab code. They consist of a

number of switch statements that selects between a number of appropriate outputs depending on the input state and can bee seen in appendix B.2.1 and B.2.2

Chapter 7

Simulation and results

7.1 Field Oriented Control

All simulations were done with a DC link voltage of $325Vdc$ an $20\mu s$ sample time, the torque is also limited to max $30Nm$. Figure 7.1 shows a simulation from stand still up to $300rad/s$ with a load of $15Nm$. The simulation consists of two phases, an accelerating part and a constant speed part. During the accelerating part the motor delivers full torque until it reaches its reference speed, the torque then drops to the same value as the load to keep the speed constant.

The simulation also shows a high ripple in both torque and current.

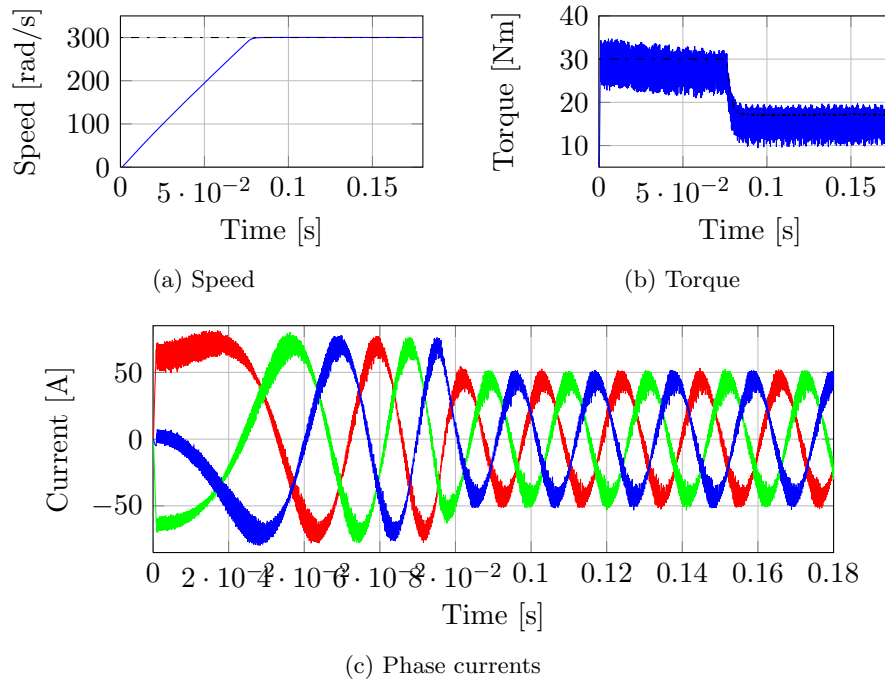


Figure 7.1: Simulation of FOC with a $15Nm$ load

Figure 7.2 shows a comparison of the reference and measured current during a linear torque ramp from $0 - 20Nm$ at a constant speed of $200rad/s$. The measured current is then normalized for comparison. It shows that the average value is approximately the same, but the current ripple for the measured one is very high.

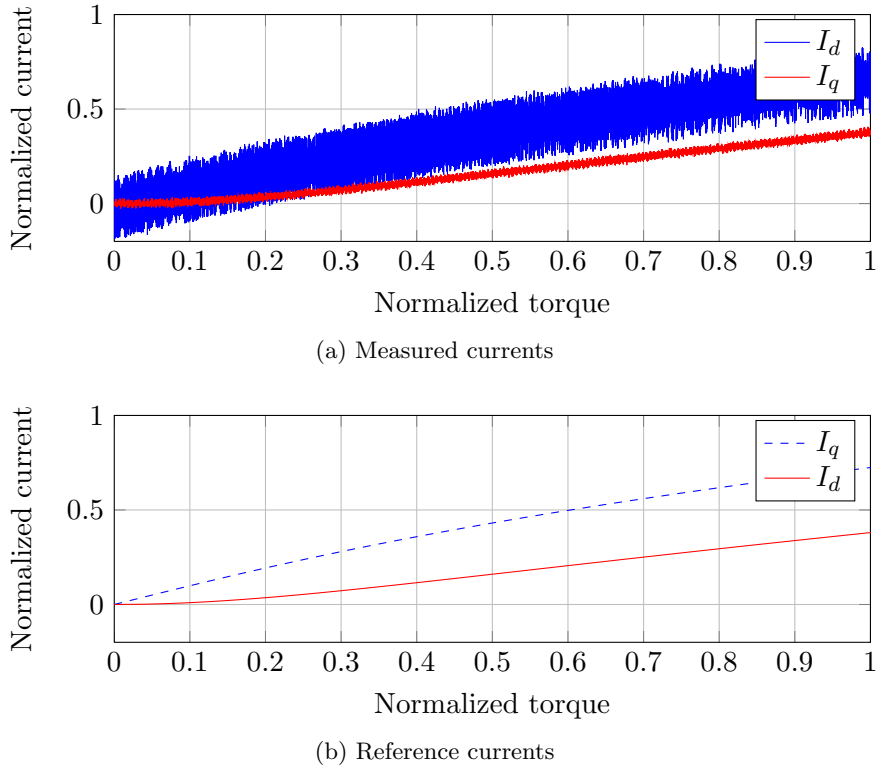


Figure 7.2: Measured and Reference currents

7.2 Direct Torque Control

The following results of the DTC are from a simulation where the motor is running at a fixed speed of 200rad/s with a 20Nm load.

Figure 7.3a show the hysteresis bands, torque and flux path for one revolution of the motor, the sample time is $20\mu\text{s}$. It can be seen that the control keeps the flux within its 0.02Wb wide hysteresis band, the torque however shows a ripple of 5Nm which is larger than the 2Nm wide hysteresis band.

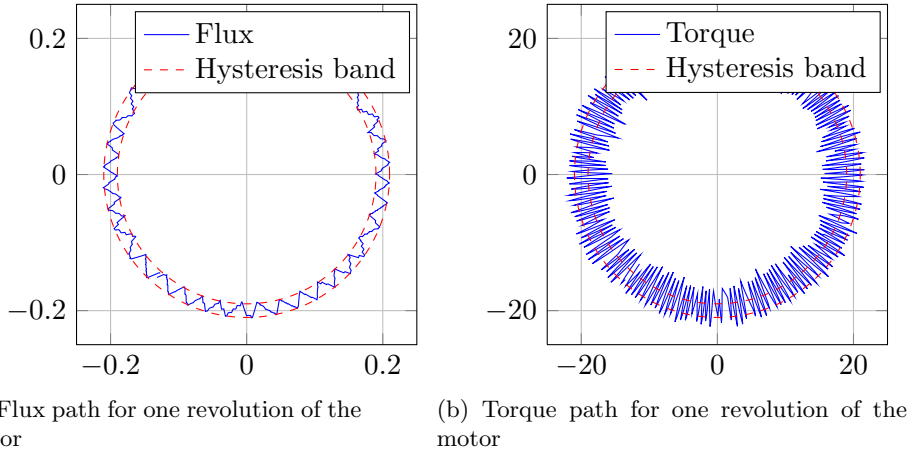


Figure 7.3: Hysteresis control with sample time of $2\mu s$

Figure 7.4 show the hysteresis bands, torque and flux path for one revolution of the motor, but with a sample time of $2\mu s$. It clearly seen that the both torque and flux is inside their limits.

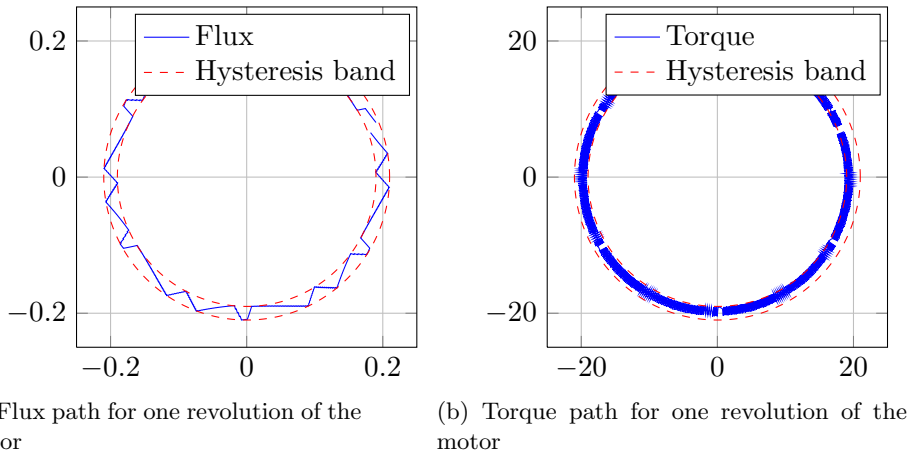


Figure 7.4: Hysteresis control with sample time of $2\mu s$

As seen in figure 7.5 the estimated sector is lagging the measured sector, at $200rad/s$ the period time is approximately $32ms$ and the time difference is between $0.6 - 0.8ms$. This corresponds to a difference in angle of $7^\circ - 9^\circ$.

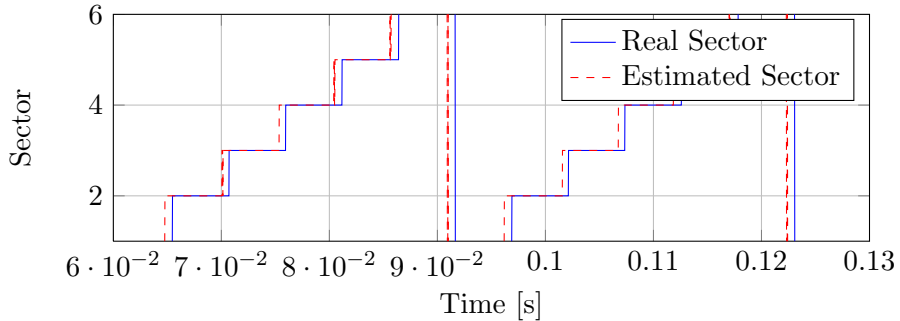


Figure 7.5: Comparison between measured and estimated sector

7.3 Comparison of FOC and DTC

To compare the two control methods they were run side by side with the same parameters, the following simulation was done with no load and with three speed steps. Figure 7.6 shows the speed reference and speed response of the motor. The two methods show no significant difference in behaviour. Figure 7.7 shows the torque produced during the run, the maximum torque

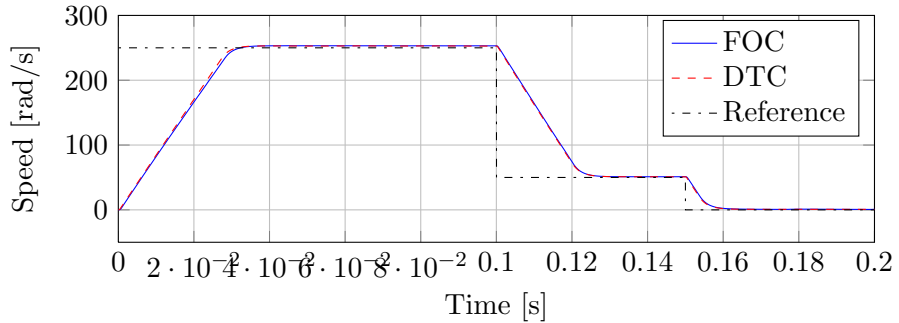


Figure 7.6: Comparison between speed response for FOC and DTC

is limited to 30Nm by the speed controller. The FOC has approximately 60% higher torque ripple than DTC during high torque operation, DTC torque ripple stays constant independent of the load situation. The torque ripple is between 15% – 30% in this case, high torque ripple is undesirable because of the strain it will put in the rest of the drive train. Figure 7.8 and 7.9 shows the phase currents for FOC respective DTC, here a significant difference between the methods can be seen. For the FOC the phase currents goes close to zero as the torque goes to zero, but for DTC the currents stay relatively high. The reason for that behaviour can be seen in figure 7.10 and 7.11

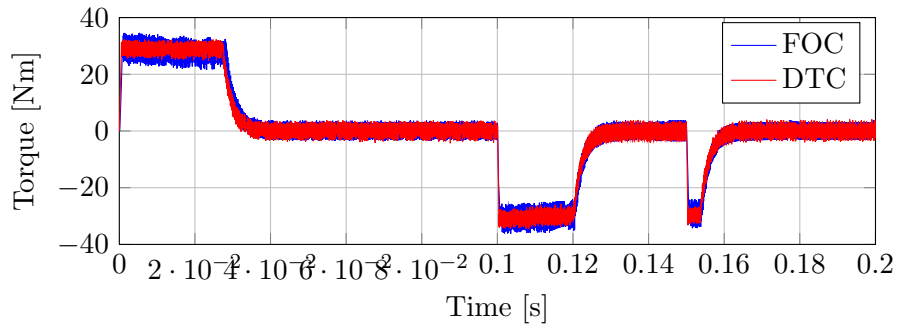


Figure 7.7: Comparison between torque response for FOC and DTC

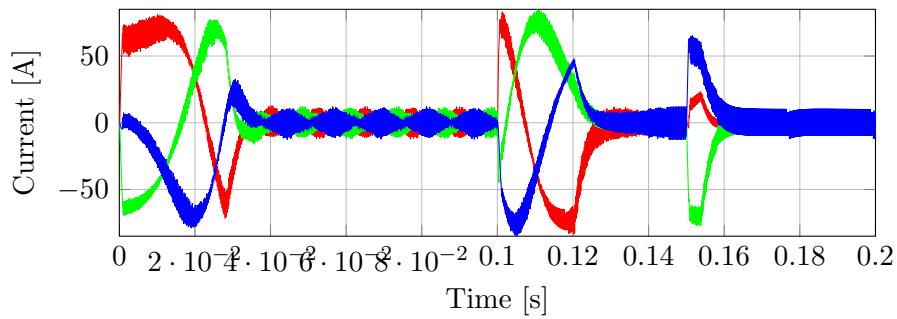


Figure 7.8: FOC phase currents

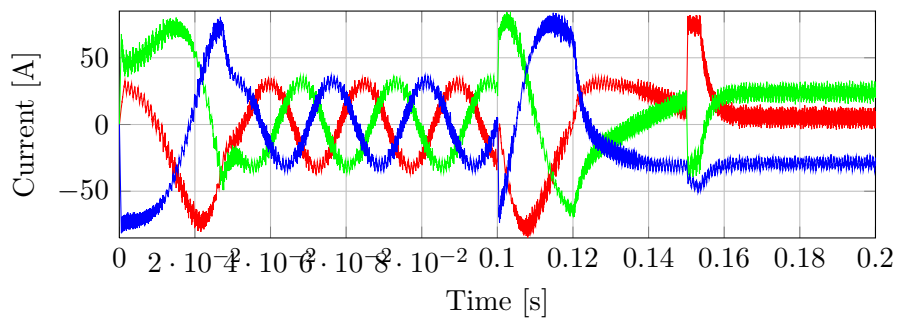


Figure 7.9: DTC phase currents

Looking at the figures it can be seen that for the DTC there is no control over the direct axis current like the FOC, and that there is a constant flow of current even as the load is zero. This is due to the constant flux reference used, it is clearly seen that a function that calculates the optimum flux dependent of the load situation has to be introduced in the model to make the drive energy efficient.

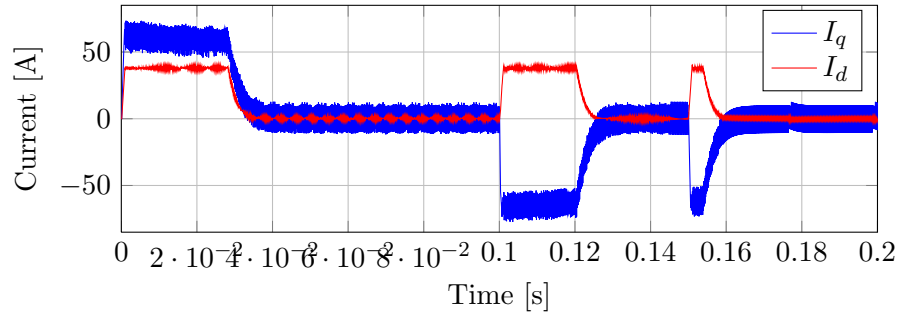


Figure 7.10: FOC dq currents

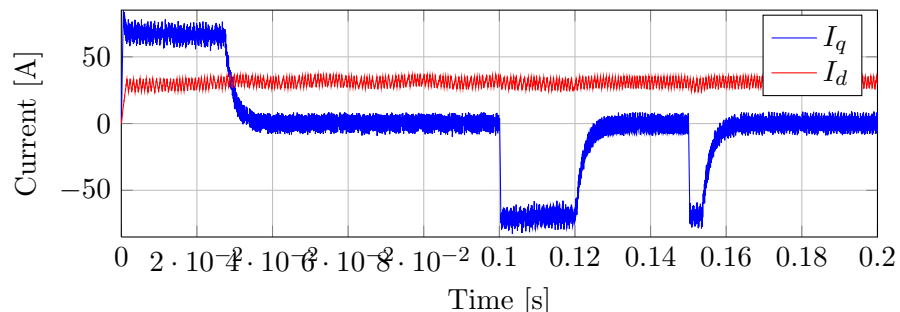


Figure 7.11: DTC dq currents

Chapter 8

Conclusion

Current control of electric motor is important not only for torque control, but also for reaching maximum efficiency. The FOC and DTC methods have been simulated and compared to find their advantages and disadvantages.

The DTC is often referred in literature as simple, which might be true for the math needed in the control systems calculations but during this project it has been quite tricky to get it to work properly. It has shown a high tendency to be very unstable, especially when considering the choice of the resistance parameter in the motor model and flux estimator. The DTC is also considered to have high torque and current ripple that can be somewhat reduced by decreasing the sample time, which has been proven to be correct. It would also be possible to reduce the ripple further by implementing some of the improvement of DTC suggested, such as Space Vector Modulation (SVM-DTC).

The FOC is normally considered to need more complex calculations to run, but with less torque and current ripple. The simulations have shown that the FOC has higher torque ripple than the DTC, but this is due to the choice to use hysteresis current control and not PI regulators. With the use of more precise current control and the use of SPWM or SVPWM it should be possible to reduce the torque ripple.

8.1 Future work

The results have shown that there are room for improvements of the models used, some of them are.

- Reduction of torque ripple for FOC, PI current controller and SPWM or SVPWM inverter switching.
- Flux calculation for DTC, to reach MTPA the flux level has to match the motors operating point.

- Reduction of torque ripple for DTC, for example implementation of SVM-DTC.
- Flux weakening of PSPMSM, for some motors and applications it might be needed to increase the motors speed range.
- New motor model and control system with a saturation model,
- Saturation, how much will the saturation affect the motor? Development of new motor model and control.
- Hardware construction of the inverter and testing/verifying the theory.

Appendix A

Derivations

A.1 Normalization of negative saliency motor

For a negative saliency pole machine the direct- and quadrature-axes inductances are unequal ($L_d < L_q$). Assuming steady state operation, the torque equation(3.20) can then be simplified to (A.1).

$$T_e = \frac{3}{2} \frac{P}{2} [\lambda_{pm} I_{sq} - (L_{mq} - L_{md}) I_{sd} I_{sq}] \quad (\text{A.1})$$

To simplify calculations it can be preferred to do them with normalized variables, to achieve this we introduce normalized variables for torque T_{en} and the direct- and quadrature- current components.

$$T_{en} = \frac{T_e}{T_{eb}} \quad (\text{A.2})$$

$$i_{qn} = \frac{i_{sq}}{i_b} \quad (\text{A.3})$$

$$i_{dn} = \frac{i_{sd}}{i_b} \quad (\text{A.4})$$

And defining base values for torque T_{eb} and current i_b .

$$i_b = \frac{\lambda_{pm}}{(L_{sq} - L_{sd})} \quad (\text{A.5})$$

$$T_{eb} = \frac{3}{2} \frac{P}{2} \lambda_{pm} i_b \quad (\text{A.6})$$

Equation (A.1) and (A.5) into (A.6) gives an expression for the normalized torque.

$$T_{en} = \frac{T_e}{T_{eb}} = \frac{\frac{3}{2} \frac{P}{2} [\lambda_{pm} I_{sq} - (L_{sq} - L_{sd}) I_{sd} I_{sq}]}{\frac{3}{2} \frac{P}{2} \lambda_{pm} i_b} =$$

$$\frac{\frac{3}{2} \frac{P}{2} [\lambda_{pm} I_{sq} - (L_{sq} - L_{sd}) I_{sd} I_{sq}]}{\frac{3}{2} \frac{P}{2} \frac{\lambda_{pm}^2}{(L_{sq} - L_{sd})}} = \frac{I_{sq}}{\frac{\lambda_{pm}}{(L_{sq} - L_{sd})}} - \frac{(L_{sq} - L_{sd}) I_{sd} I_{sq}}{\frac{\lambda_{pm}^2}{(L_{sq} - L_{sd})}} \Leftrightarrow$$

$$T_{en} = \frac{I_{sq}}{i_b} \left(1 - \frac{I_{sd}}{i_b} \right) \quad (\text{A.7})$$

Which gives normalized electromechanical torque.

$$T_{en} = i_{qn}(1 - i_{dn}) \quad (\text{A.8})$$

By rearranging (A.8) we can plot the constant torque loci, see Figure 5.1.

$$i_{qn} = \frac{T_{en}}{1 - i_{dn}} \quad (\text{A.9})$$

or

$$i_{dn} = 1 - \frac{T_{en}}{i_{qn}} \quad (\text{A.10})$$

To reach maximum efficiency of the machine , you would like maximize the torque per ampere relationship (MPTA). This is done by minimizing the distance from origin to the torque locus of desired torque, which gives the minimum stator current for a specified reference torque.

$$i_n^2 = i_{dn}^2 + i_{qn}^2 = i_{dn}^2 + \left(\frac{T_{en}}{1 - i_{dn}} \right)^2 \quad (\text{A.11})$$

or

$$i_n^2 = i_{dn}^2 + i_{qn}^2 = \left(1 - \left(\frac{T_{en}}{i_{qn}} \right) \right)^2 + i_{qn}^2 \quad (\text{A.12})$$

By differentiating (A.11) with respect to i_{dn} and setting the result to zero, the relationship between torque- and direct-axis current-references can be obtained.

$$\frac{\partial i_n^2}{\partial i_{dn}} = 2I_{dn} - 2 \frac{T_{en}^2}{(i_{dn} - 1)^3} = 0 \Rightarrow \quad (\text{A.13})$$

$$T_{en}^* = \sqrt{i_{dn}^* (i_{dn}^* - 1)^3} \quad (\text{A.14})$$

Or from (A.12) the relationship between torque- and quadrature-axis current-references can be obtained.

$$\frac{\partial i_n^2}{\partial i_{qn}} = 2i_{qn} - \frac{2T_{en} \left(\frac{T_{en}}{i_{qn}} - 1 \right)}{i_{qn}^2} = 0 \Rightarrow \quad (\text{A.15})$$

$$T_{en}^* = \frac{i_{qn}^*}{2} \left(1 + \sqrt{1 + 4(i_{qn}^*)^2} \right) \quad (\text{A.16})$$

To be able to get the reference currents, equation (A.14) or (A.16) has to be solved. The solution of (A.16) for i_{qn} is.

$$i_{qn} = \frac{1}{2}\sqrt{A + B - C} - \frac{1}{2}\sqrt{D} \quad (\text{A.17})$$

Where:

$$\begin{aligned} A &= \frac{4\sqrt[3]{\frac{2}{3}T_{en}^2}}{\sqrt[3]{9T_{en}^2 + \sqrt{3}\sqrt{256T_{en}^6 + 27T_{en}^4}}} \\ B &= \frac{2T_{en}}{\sqrt{\frac{\sqrt[3]{9T_{en}^2 + \sqrt{3}\sqrt{256T_{en}^6 + 27T_{en}^4}}}{\sqrt[3]{23^{\frac{2}{3}}}} - \frac{4\sqrt[3]{\frac{2}{3}T_{en}^2}}{\sqrt[3]{9T_{en}^2 + \sqrt{3}\sqrt{256T_{en}^6 + 27T_{en}^4}}}}} \\ C &= \frac{\sqrt[3]{9T_{en}^2 + \sqrt{3}\sqrt{256T_{en}^6 + 27T_{en}^4}}}{\sqrt[3]{23^{\frac{2}{3}}}} \\ D &= \frac{\sqrt[3]{9T_{en}^2 + \sqrt{3}\sqrt{256T_{en}^6 + 27T_{en}^4}}}{\sqrt[3]{23^{\frac{2}{3}}}} - \frac{4\sqrt[3]{\frac{2}{3}T_{en}^2}}{\sqrt[3]{9T_{en}^2 + \sqrt{3}\sqrt{256T_{en}^6 + 27T_{en}^4}}} \end{aligned}$$

The direct axis current reference can then be calculated with equation (A.10) from the reference torque and quadrature axis current.

A.2 Normalization of positive saliency motor

For a positive saliency pole machine the direct- and quadrature-axes inductances are unequal ($L_d > L_q$). The derivation follows the same steps as in appendix A.1, but with a different base current

$$i_b = \frac{\lambda_{pm}}{(L_{sd} - L_{sq})} \quad (\text{A.18})$$

Which gives the normalized torque.

$$T_{en} = i_{qn}(1 + i_{dn}) \quad (\text{A.19})$$

By rearranging (A.19) we can plot the constant torque loci, see figure 5.3

$$i_{qn} = \frac{T_{en}}{1 + i_{dn}} \quad (\text{A.20})$$

or

$$i_{dn} = \frac{T_{en}}{i_{qn}} - 1 \quad (\text{A.21})$$

And the torque as a function of direct- and quadrature-currents will be.

$$T_{en}^* = \sqrt{i_{dn}^* (i_{dn}^* + 1)^3} \quad (\text{A.22})$$

$$T_{en}^* = \frac{i_{qn}^*}{2} \left(1 + \sqrt{1 + 4(i_{qn}^*)^2} \right) \quad (\text{A.23})$$

Since equation (A.23) and (A.16) are the same, equation (A.17) is valid also for a positive saliency motor. But the direct axis current is not the same and has to be calculated from equation (A.21).

A.3 Polar coordinates

The magnitude of the stator armature current I_s can be expressed as function of the direct and quadrature axis currents I_d and I_q .

$$|I_s| = \sqrt{I_d^2 + I_q^2} \leq I_{sm} \quad (\text{A.24})$$

The direct and quadrature axis currents can be expressed as a function of armature current and its angle α .

$$I_d = |I_s| \cos(\alpha) \quad (\text{A.25})$$

$$I_q = |I_s| \sin(\alpha) \quad (\text{A.26})$$

$$\alpha = \arctan\left(\frac{I_q}{I_d}\right) \quad (\text{A.27})$$

From (A.25) and (A.26) into the torque equation(3.20) we get.

$$\begin{aligned} T_e &= \frac{3}{2} \frac{P}{2} [\lambda_{pm}|I_s| \sin(\alpha) + (L_d - L_q)|I_s|^2 \sin(\alpha) \cos(\alpha)] \Leftrightarrow \\ T_e &= \frac{3}{2} \frac{P}{2} \left[\lambda_{pm}|I_s| \sin(\alpha) + (L_d - L_q)|I_s|^2 \frac{1}{2} \sin(2\alpha) \right] \end{aligned} \quad (\text{A.28})$$

By differentiating (A.28) with respect to α and setting the result to zero, we get an equation for the Maximum Torque Per Ampere trajectory.

$$\frac{\partial T_e}{\partial \alpha} = \frac{3}{2} \frac{P}{2} [\lambda_{pm}|I_s| \cos(\alpha) + (L_d - L_q)|I_s|^2 \cos(2\alpha)] = 0 \quad (\text{A.29})$$

From (A.25) and (A.26) into (A.29) we get

$$\begin{aligned} \frac{3}{2} \frac{P}{2} [\lambda_{pm}|I_s| \cos(\alpha) + (L_d - L_q)|I_s|^2 (\cos^2(\alpha) - \sin^2(\alpha))] &= 0 \Leftrightarrow \\ \lambda_{pm}I_d + (L_d - L_q)I_d^2 - (L_d - L_q)I_q^2 &= 0 \end{aligned} \quad (\text{A.30})$$

From (A.30) we get

$$I_d = -\frac{\lambda_m}{2(L_d - L_q)} + \sqrt{\frac{\lambda_m^2 + 4I_q^2L_d^2 - 8I_qL_dL_q + 4I_q^2L_q^2}{4(L_d - L_q)^2}} \Leftrightarrow$$

$$I_d = -\frac{\lambda_m}{2(L_d - L_q)} + \sqrt{\frac{\lambda_m^2}{4(L_d - L_q)} + I_q^2} \quad (\text{A.31})$$

To eliminate i_q , equation (A.24) is used

$$I_d = -\frac{\lambda_m}{2(L_d - L_q)} + \sqrt{\frac{\lambda_m^2}{4(L_d - L_q)} + |I_s|^2 - I_d^2}$$

Then solving for I_d , we get I_d as a function of $|I_s|$

$$I_d = -\frac{\lambda_m}{4(L_d - L_q)} + \sqrt{\frac{8|I_s|^2(L_d - L_q)^2 + \lambda_m^2}{16(L_d - L_q)^2}} \Leftrightarrow$$

$$I_d = -\frac{\lambda_m}{4(L_d - L_q)} + \sqrt{\frac{\lambda_m^2}{16(L_d - L_q)^2} + \frac{|i_{sm}|^2}{2}} \quad (\text{A.32})$$

And I_q is obtained from equation (A.24)

$$I_q = \sqrt{|i_s|^2 - i_d^2} \quad (\text{A.33})$$

Appendix B

Simulink model

B.1 Field Oriented Control Schematics

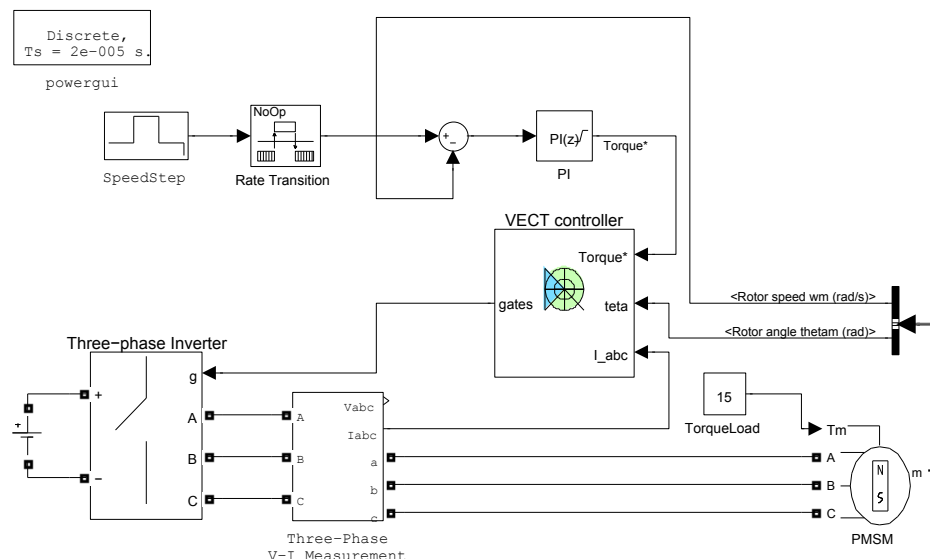


Figure B.1: Main controller

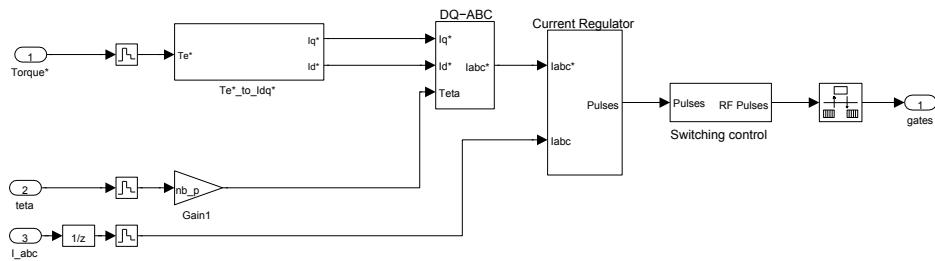


Figure B.2: Current controller / VECT controller

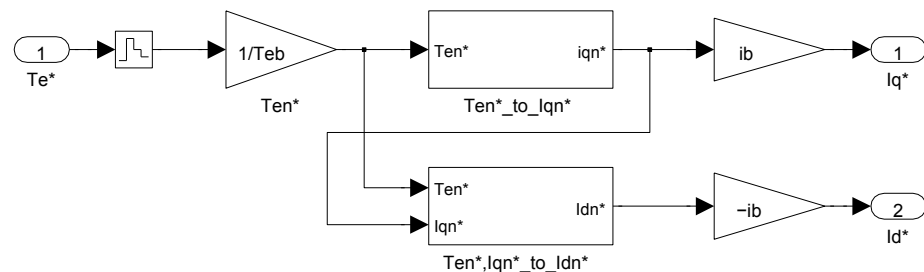


Figure B.3: Torque to currents

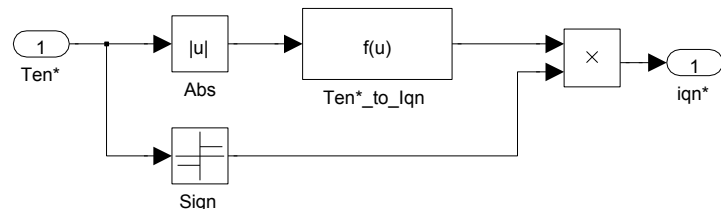


Figure B.4: Torque to quadrature axis current

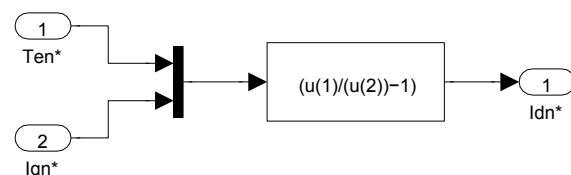


Figure B.5: Torque to direct axis current

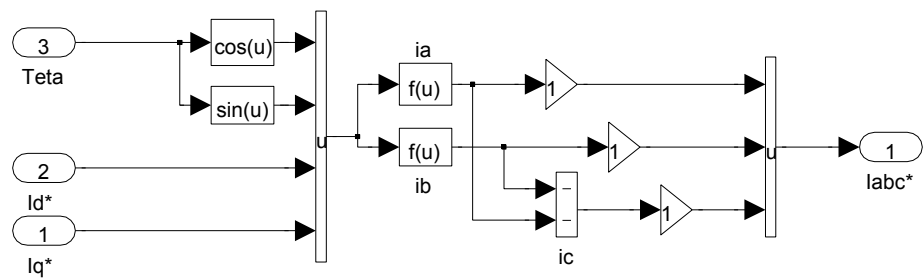


Figure B.6: Direct- and Quadrature-axis currents to ABC currents

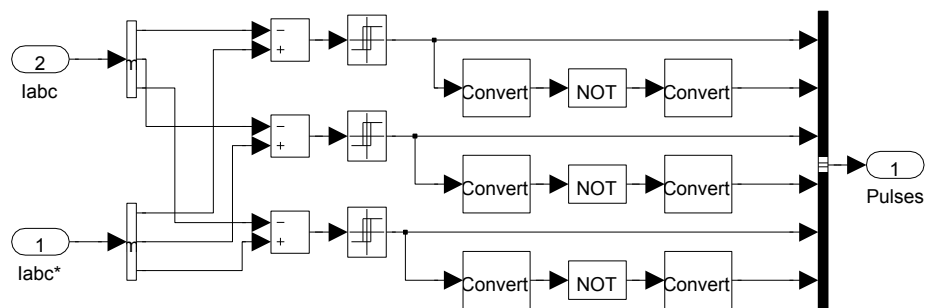


Figure B.7: Current regulator

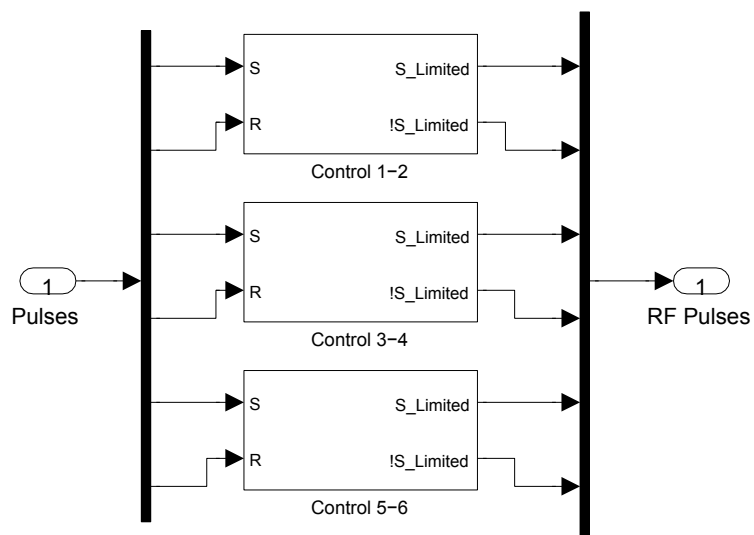


Figure B.8: Pulse generator

B.2 Direct Torque Control Schematics

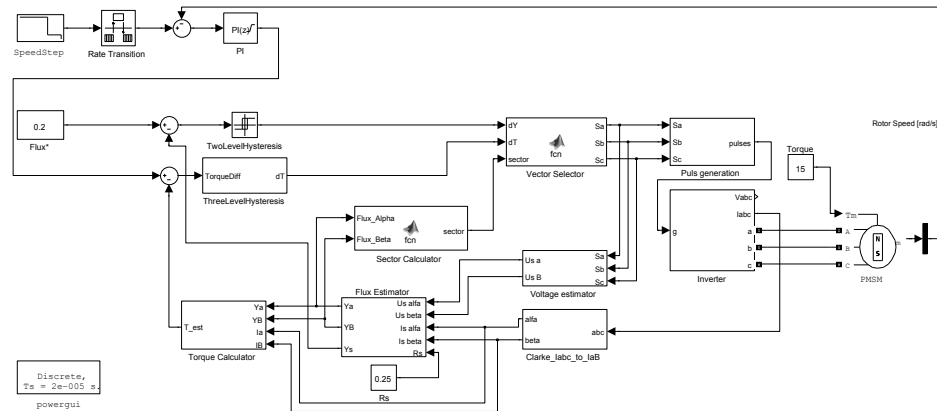


Figure B.9: Main controller

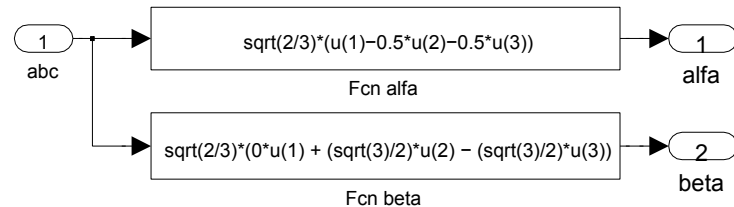


Figure B.10: Clarke current transformation

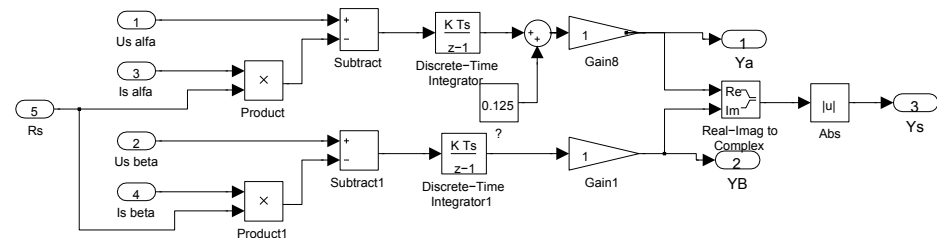


Figure B.11: Flux estimator

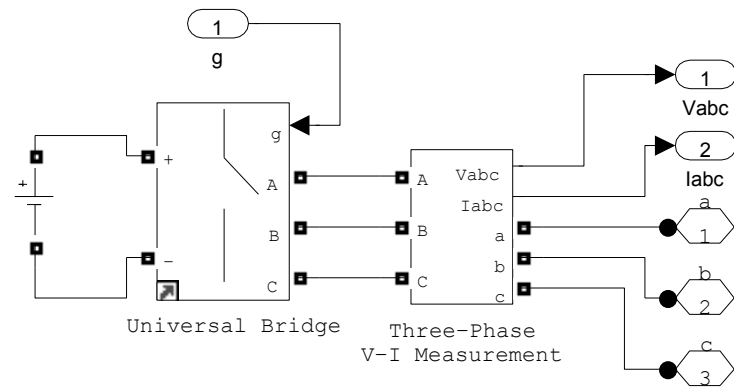


Figure B.12: Two level inverter

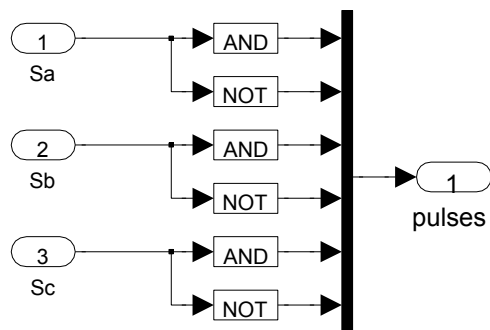


Figure B.13: Pulse generator

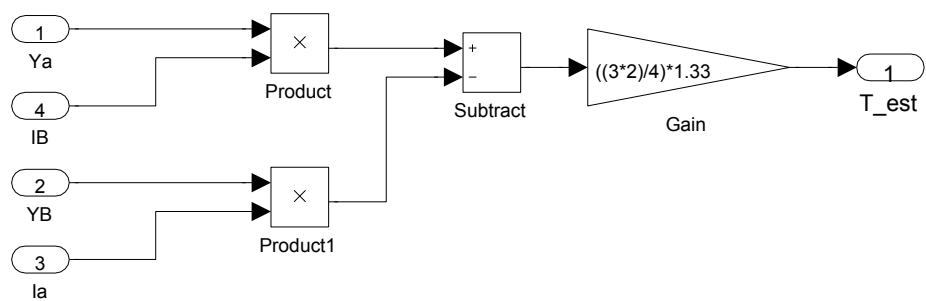


Figure B.14: Torque calculator

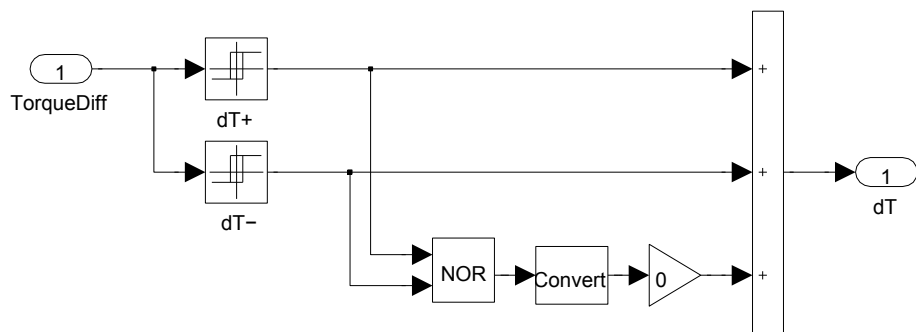


Figure B.15: Torque hysteresis comparator

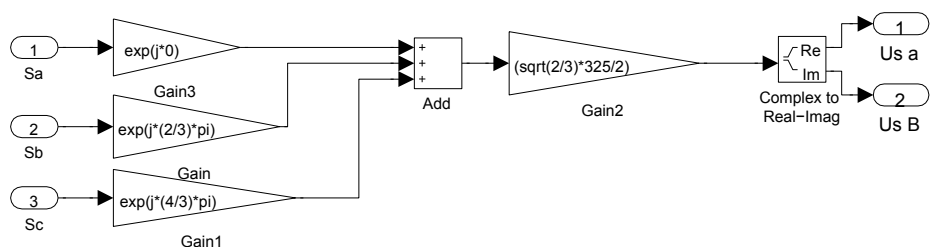


Figure B.16: Voltage estimator, without losses in inverter switches

B.2.1 Matlab code for Sector calculation

```
1 function sector = fcn(Flux_Alpha, Flux_Beta)
2 sector = 0;
3 theta=(180/pi)*atan2(Flux_Beta, Flux_Alpha);
4 if theta ≥ -30 && theta < 30
5     sector = 1;
6 end
7 if theta ≥ 30 && theta < 90
8     sector = 2;
9 end
10 if theta ≥ 90 && theta < 150
11     sector = 3;
12 end
13 if theta ≥ 150 || theta < -150
14     sector = 4;
15 end
16 if theta ≥ -150 && theta < -90
17     sector = 5;
18 end
19 if theta ≥ -90 && theta < -30
20     sector = 6;
21 end
```

B.2.2 Matlab code for Vector selection

```
1 function [Sa,Sb,Sc] = fcn(dY, dT, sector)
2 vector = 0;
3 temp = [0 0 0];
4 switch dY %————— dY = 1
5     case 1
6         switch dT
7             case 1
8                 switch sector % dY = 1, dT = 1
9                     case 1
10                         vector = 2;
11                     case 2
12                         vector = 3;
13                     case 3
14                         vector = 4;
15                     case 4
16                         vector = 5;
17                     case 5
18                         vector = 6;
19                     case 6
20                         vector = 1;
21                 end
22             case 0
23                 switch sector % dY = 1, dT = 0
24                     case 1
25                         vector = 0;
```

```

26         case 2
27             vector = 7;
28         case 3
29             vector = 0;
30         case 4
31             vector = 7;
32         case 5
33             vector = 0;
34         case 6
35             vector = 7;
36     end
37 case -1
38     switch sector % dY = 1, dT = -1
39         case 1
40             vector = 6;
41         case 2
42             vector = 1;
43         case 3
44             vector = 2;
45         case 4
46             vector = 3;
47         case 5
48             vector = 4;
49         case 6
50             vector = 5;
51     end
52 end
53 case -1 % _____ dY = -1
54     switch dT
55         case 1
56             switch sector % dY = -1, dT = 1
57                 case 1
58                     vector = 3;
59                 case 2
60                     vector = 4;
61                 case 3
62                     vector = 5;
63                 case 4
64                     vector = 6;
65                 case 5
66                     vector = 1;
67                 case 6
68                     vector = 2;
69             end
70         case 0
71             switch sector % dY = -1, dT = 0
72                 case 1
73                     vector = 7;
74                 case 2
75                     vector = 0;
76                 case 3
77                     vector = 7;
78                 case 4
79                     vector = 0;

```

```

80         case 5
81             vector = 7;
82         case 6
83             vector = 0;
84     end
85 case -1
86     switch sector % dY = -1, dT = -1
87         case 1
88             vector = 5;
89         case 2
90             vector = 6;
91         case 3
92             vector = 1;
93         case 4
94             vector = 2;
95         case 5
96             vector = 3;
97         case 6
98             vector = 4;
99     end
100 end
101
102
103 % Select switch positions
104 switch vector
105     case 0
106         temp = [0 0 0];
107     case 1
108         temp = [1 0 0];
109     case 2
110         temp = [1 1 0];
111     case 3
112         temp = [0 1 0];
113     case 4
114         temp = [0 1 1];
115     case 5
116         temp = [0 0 1];
117     case 6
118         temp = [1 0 1];
119     case 7
120         temp = [1 1 1];
121 end
122 Sa = temp(1);
123 Sb = temp(2);
124 Sc = temp(3);

```

Bibliography

- [1] J.F. Gieras. *Permanent magnet motor technology: design and applications*. Electrical and Computer Engineering Series. CRC Press, 2009. ISBN 9781420064407. URL <http://books.google.se/books?id=8b6yPQAACAAJ>.
- [2] Juha Pyrhönen. Electrical drives - lecture notes, 2011.
- [3] Boel Ekergård. 2012.
- [4] Nicola Bianchi, Silverio Bolognani, and Brian J. Chalmers. Salient-rotor pm synchronous motors for an extended flux-weakening operation range. *IEEE Transaction on industry applications*, 36(4):1118–1125, 2000.
- [5] Roberto H. Moncada, Juan A. Tapia, and Thomas M. Jahns. Inverse-saliency pm motor performance under vector control operation. *IEEE Energy Conversion Congress and Exposition*, pages 2368–2373, 2009.
- [6] Roberto H. Moncada, Juan A. Tapia, and Thomas M. Jahns. Analysis of negative-saliency permanent-magnet machines. *IEEE transactions on industrial electronics*, 57(1):122–127, 2010.
- [7] M. Leijon, B. Ekergård, S. Ferhatovic, J. de Santiago, H. Bernhoff, R. Waters, and S. Eriksson. On a two pole motor for electric propulsion system. 2012.
- [8] B. Bolund, M. Leijon, and U. Lundin. Poynting theorem applied to cable wound generators. *IEEE Transaction on Dielectrics and Electrical Insulation*, 15(2):600–605, 2008.
- [9] J.J. Grainger and W.D. Stevenson. *Power system analysis*. McGraw-Hill series in electrical and computer engineering: Power and energy. McGraw-Hill, 1994. ISBN 9780070612938. URL <http://books.google.se/books?id=NBIoAQAAQAAJ>.
- [10] H.A. Toliyat and S.G. Campbell. *DSP-Based electromechanical motion control*. Power electronics and applications series. CRC Press,

2004. ISBN 9780849319181. URL <http://books.google.se/books?id=3MgkRkPi3k4C>.

- [11] P.D. Chandana Perera, F. Blaabjerg, J.K. Pedersen, and P. Thogersen. A sensorless, stable v/f control method for permanent-magnet synchronous motor drives. *IEEE Transaction on industry applications*, 39(3):83–89, 2003.
- [12] R.S. Colby and D.W. Novotny. An efficiency-optimizing permanent-magnet synchronous motor drive. *IEEE Transaction on industry applications*, 24(3):462–496, 1988.
- [13] Y. Nakamura, T. Kudo, F. Ishibashi, and S. Hibino. High-efficiency drive due to power factor control of a permanent magnet synchronous motor. *IEEE Transaction on power electronics*, 10(2):247–253, 1995.
- [14] Thomas M. Jahns, Gerald B. Kliman, and Thomas W. Neumann. Interior permanent-magnet synchronous motors for adjustable-speed drives. *IEEE Transaction on industry applications*, IA-22(4):738–747, 1986.
- [15] R.D. Doncker, D.W.J. Pulle, and A. Veltman. *Advanced Electrical Drives: Analysis, Modeling, Control*. Power Systems. Springer, 2011. ISBN 9789400701793. URL http://books.google.se/books?id=_sEDx21AKboC.
- [16] Isao Takahashi and Toshihiko Noguchi. A new quick-response and high-efficiency control strategy of an induction motor. *IEEE Transaction on industry applications*, IA-22(5):820–827, 1986. Original article in japanese.
- [17] M. Depenbrock. Direct self-control (dsc) of inverter-fed induction machine. *IEEE Transaction on power electronics*, 3(4):420–429, 1988. Original article in german.
- [18] Jukka Kaukonen. *Salient Pole Synchronous Macine Modelling in a Industrial Direct Torque Controlled Drive Application*. PhD thesis, Lappeenranta University of Technology, 1999.
- [19] Xing Shaobang, Luo Yinsheng, and Han Xiaoxin. Efficiency improvement on pmsm twelve sectors dtc system. *Control and Decision Conference*, pages 1208–1212, 2011.
- [20] Yi Wang and Jianguo Zhu. Modelling and implementation of an improved dsvm scheme for pmsm dtc. *International Conference on Electrical Machines and Systems*, pages 1042–1046, 2008.
- [21] H. Ziane, J.M. Retif, and T. Rekioua. Fixed-switching-frequency dtc control for pm synchronous machine with minimum torque ripples.

Canadian Journal of Electrical and Computer Engineering, 33(3):183–189, 2008.

- [22] B. Bossoufi, M. Karim, A. Lagrioui, and S. Ioniță. Performance analysis of direct torque control (dtc) for synchronous machine permanent magnet (pmsm). *2010 IEEE 16th International Symposium for Design and Technology in Electronic Packaging (SIITME)*, pages 237–242, 2010.